LUND UNIVERSITY

WIND-INDUCED TRANSMISSION OF LOW FREQUENCY VIBRATIONS FOR A TALL MULTI-STOREY WOOD BUILDING

GUSTAV SPJUTH and LOUISE ÅKESSON

Engineering Acoustics

Master's Dissertation

DEPARTMENT OF CONSTRUCTION SCIENCES

DIVISION OF ENGINEERING ACOUSTICS

ISRN LUTVDG/TVBA--16/5050--SE (1-77) | ISSN 0281-8477

MASTER'S DISSERTATION

WIND-INDUCED TRANSMISSION OF LOW FREQUENCY VIBRATIONS FOR A TALL MULTI-STOREY WOOD BUILDING

GUSTAV SPJUTH and LOUISE ÅKESSON

Supervisors: **DELPHINE BARD**, Assoc. Prof. and **JUAN NEGREIRA**, PhD,
Div. of Engineering Acoustics, LTH, Lund.

Examiner: Professor **KENT PERSSON**, Div. of Structural Mechanics, LTH, Lund.

Printed by Media-Tryck LU, Lund, Sweden, November 2016 *(Pl)*.

For information, address:
Division of Engineering Acoustics,
Faculty of Engineering LTH, Lund University, Box 118, SE-221 00 Lund, Sweden.
Homepage: www.akustik.lth.se

Abstract

The building industry accounts for a large part of the world's carbon dioxide emissions. At the same time the awareness of sustainable construction and production phase has increased and focus has been directed towards the material wood. Likewise, continuing urbanisation requires multi-storey buildings made of wood which brings along certain difficulties and challenges. Due to the low mass of wood, the structural stiffness is less than that of a similar concrete building. On top of that, vibrations that are induced by wind are easily transmitted through the construction. Even if lightweight constructions comply to the present regulations, acoustic comfort is sometimes not met and complaints from residents arise.

This thesis investigates if people could be affected by building vibrations and the sound generated by different types of loads, e.g. wind loads. This is done by creating a predictive modelling approach with available prediction tools. The model is not calibrated against any measurements, but for the design of the structure, an example case is used, namely Wood Innovation and Design Centre. This existing structure is seven storeys high and made of wood. The building is designed by Michael Green Architecture and one of their goals is to build a 30-storey or taller wood building.

To estimate noise and vibration levels, a finite element model of the aforementioned building is created with 32 storeys. Only wind-induced noise radiated from the enclosing surfaces of a room is analysed. Several parametric tests are performed both to assure the accuracy of the model, and to investigate the most severe sound pressure levels and vibrations occurring in the building. The studies are limited to the low-frequency range from 0 up to 100 Hz.

The main conclusion from this thesis is that, for the case under study, the sound pressure level caused by vibrations induced by the wind load itself is not likely to exceed the audible threshold. In an unlikely case with high wind density in frequencies above 50 Hz, i.e. when the excitation force includes large amplitudes at frequencies above 50 Hz, and under certain modelling conditions i.e. fixed connections, could the audible threshold be exceeded. This does not conclude that wind load can not create noise being audible from other types of interactions, such as rattling sound, windows, turbulence due to the building shape, etc.

The model in this thesis shows that the recommended vibration levels are exceeded in both the horizontal and the vertical direction, which indicates that people inside of this building probably will be affected by the vibrations. The highest accelerations appear on the top floor for both directions whereas the room placement only is of importance for vibrations in the vertical direction.

As this thesis is just touching the possibilities of these modelling tools, more could be explored in the use of acoustic media, submodels and wind load analyses.

Keywords: acoustic, CLT, FEM, multi-storey, radiation, SPL, vibrations, WIDC.

Acknowledgements

This master thesis was carried out at the Division of Engineering Acoustics, Faculty of Engineering LTH at Lund University during 2016.

The authors express their thanks to the supervisors Dr. Sc. Delphine Bard and Ph.D Juan Negreira which made this thesis possible. Special thanks to Juan Negreira which constantly boosted our spirits and helped with a little bit of every thing in difficult times.

We would also give our gratitude to Michael Green and Michael Green Architecture which gave us access to the reference building *Wood Innovation and Design Centre* and the elementary sketches of the project.

We would also thanks our families for the support during the whole project.

Gustav Spjuth and Louise Åkesson, Lund, November 2016

Contents

List of Figures

List of Tables

1
Introduction

1.1 Background

The building industry accounts for a large part of the world's carbon dioxide emissions. At the same time the awareness of sustainable construction and production phase has increased and focus has been directed towards the material wood. Likewise, continuing urbanisation requires multi-storey buildings made of wood which brings along certain difficulties and challenges. Due to the low mass of wood, the structural stiffness is less than that of a similar concrete building. On top of that, vibrations that are induced by e.g. wind or from the traffic are easily transmitted through the construction. Even if lightweight constructions comply to the present regulations, acoustic comfort is sometimes not met and complaints from inhabitants arise.

Usually, wood behaves fairly good when it comes to vibratory and acoustic performance at high frequencies [1]. One of the main weaknesses for wood is its poor sound insulation in the low frequency range. How well the sound transmit depends on the frequency of the sound and the weight of the material [1].

Tall wood buildings are raising all over the world and the competition of the tallest wood building is constantly ongoing. The data material in this master thesis comes from Michael Green Architecture. It is a company that today has an existing 29.3 meters high 7-storey wood building, *Wood Innovation and Design Centre*, WIDC. The latter building is used as an example case for the work performed. One of their goals is to reach a 30-storey wood building, which then will be the highest in the world. Problems that could arise when constructing tall wood buildings are for instance concerning strength, fire safety, and acoustic performance [2].

The regulations for sound insulation differ depending on what country and type of room it is designed for. In Sweden the lowest frequency range covers down to 50 Hz when analysing impact sound and airborne sound [3]. These criteria restrict the building to fulfil the standards, both for the floors and walls. The criterion range does not complete the hearing range and has lack of restrictions which are causing problems in the lower frequencies, which especially affects wooden buildings. Due to the current restrictions this could lead to unwanted noise even though the criterion is fulfilled. The human perception vary a lot from person to person, which makes it difficult when setting up regulations. Moreover, the hearing range is often said to

be between 20 Hz to 20 000 Hz in which both vibrations and acoustic phenomena could occur.

Nowadays, prediction tools for wooden buildings are few, and they are mostly based on measurements performed on existing buildings and engineering experience. Finite element models, i.e. FE models, would entail time and cost savings for industry, but due to the complexity of acoustic phenomena these are still hard to create and evaluate.

1.2 Aim and objective

The aim of this master thesis is to find out if wind-induced vibrations and noise in a tall wood building are affecting the residents. The thesis investigates vibrations and the sound generated by means of numerical tools. The master thesis also proposes a methodology on how to model tall buildings using FEM in a time-efficient and accurate way.

The objective is thus two-fold:

- get an indication, for the model under consideration, of the values for the sound pressure level which could take place within the building caused by a wind load for frequencies below 100 Hz,
- predict and compare vibrations occurring in the building with current restrictions.

A FE model based on the structure of an existing wood building is modelled to a taller building. When the model is set up, an implementation of acoustic media is introduced to enable sound pressure levels to be retrieved.

1.3 Research limitations and assumptions applied

In the modelling of the tall wood building dealt with in the master thesis, several limitations and assumptions have been made.

- Connections are simplified to fixed joints.
- Damping is set to a realistic value obtained from measurements in a similar existing building.
- The complete building is supposed to stand alone, i.e no shielding from other buildings is accounted for.
- No comparison with measurements is performed.
- Studies are limited to the low-frequency range, from 0 up to 100 Hz.
- Loads of low magnitude suppose to give linear elastic material response.
- Long wavelengths in comparison with material heterogeneities allow materials to be modelled homogeneous.

2
Wood

Wood is a renewable, environmentally friendly and sustainable resource which makes it an attractive material for green building construction. Its ability to absorb carbon dioxide during its growth can make up for the carbon dioxide emissions caused by its production, making timber nearly carbon neutral [4]. According to Svenskt Trä [4] approximately 17 million m^3 of timber were produced under the last 10 years in Sweden. Around two thirds of this was exported to other countries.

Unlike concrete and steel, wood is an anisotropic material, which means that it has different material properties in different directions as seen in figure 2.1. For example, the tensile strength parallel to the grain is much higher than the compressive strength and an increasing moisture content will decrease the strength until the fibre saturation point has been reached [5]. Due to growth irregularities such as knots, cracks and resin pockets, every piece of wood is unique, which makes the load-bearing capacity hard to establish [6]. Research and development have led to great improvements of wood structures with regard to fire safety and sound insulation [7]. Using wood composite materials, such as cross-laminated timber, is a way to increase the load-bearing capacity and satisfy modern criteria [8].

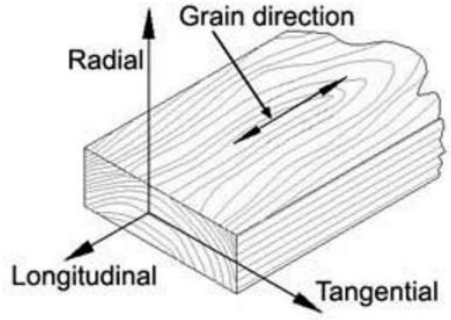

Figure 2.1. Principal directions of wood [9].

2.1 Cross-Laminated Timber (CLT)

Cross-laminated timber, CLT, is structured with glue adhered massive wood layers rotated 90° with respect to the adjacent layer, i.e. in different grain directions, in order to increase the strength in several directions. The number of layers depends of the use of the part, but usually this number is uneven and range from 3 to 9.

The orthogonal symmetry increase the stiffness and strength both parallel and perpendicular to the grain which makes CLT a good construction material [7]. Other benefits of CLT are its stabilising capacity, acoustic insulation capacity, heat insulation capacity and fire protection capacity, and that it moisture controls the indoor air [10]. Off-site prefabrication shortens the assembly time [8].

The complicated structure of wood makes it hard to model. Therefore wood is often simplified into an orthotropic material. This means that instead of three different strength directions only two are considered; one parallel to the grain direction and one perpendicular to it. When using CLT-panels the parallel grain direction is stronger and the number of layers determines how the strength is distributed. Figure 2.2 shows a CLT cross-section.

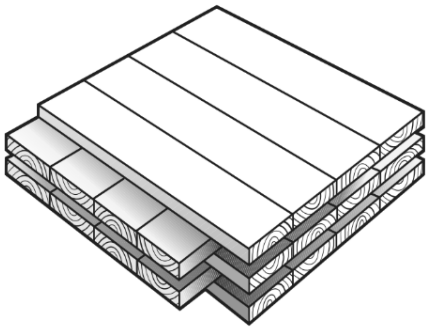

Figure 2.2. Example of a CLT Cross-Section [11].

2.2 Acoustic insulation properties

Wood is not only an esthetically appealing material, but may even be desirable in order to create a well-functioning acoustic environment. For instance, concert halls are often using wood panels to control the propagating sound to the audience and wood could also work well as an acoustic resonance box for musical instruments. Wood is a relatively hard material and therefore has an reflective surface which makes it to a less good sound absorbent [12].

Building acoustics is often focusing on keeping sound from transmitting into a room and maintaining the sound environment. For a room to fulfil good sound reduction, generally heavier materials are desirable. With wood being a light construction material, it therefore needs to be compensated against weight and total mass. For example, several layers of wood could be used or other materials mixed in. CLT consists of several layers of wood and therefore it is heavier than a single wood frame, the volume is larger and therefore sometimes hard to fit in. Even if the mass is important for the sound reducing ability, wood is used in studs and interior walls. Because sound propagates faster in wood compared to air, the wood could act as a sound bridge [13]. If the studs in the interior walls are divided into two separated systems, the sound reduction will increase. As previously mentioned, wood is not

optimal in the use of an absorbent and therefor it should be supplemented by, for example, mineral wool insulation or some other typical sound absorbing material [13].

When wood is used as a structural system, there are risks that vibrations and low frequent sounds propagate between different rooms. Wood itself has a relatively good ability to damp medium and high frequencies, but it is often discussed as week in the low frequency register [1]. When wood has difficulties to reduce the lower frequencies it means that, for instance, step sound and noise from machinery easier spread in a wood building compared to a concrete building [13]. More about the acoustical terms and definitions are explained in chapter 4.

3
Wind

In densely built up areas tall buildings are exposed to wind loads which can be challenging both from a structural as well as a vibroacoustic point of view. For most tall buildings, it is the design and not the strength that is regulated by the serviceability considerations [14], due to humans being sensitive to vibrations. Wind pressure makes resilient lightweight structures move from side to side, causing accelerations that can have negative impact on the people living or working inside of the building, such as nausea [15].

The magnitude of wind loading depends on the wind speed and the structure's shape, height and topographic location. If other buildings and obstacles of great height are close to the building, these may cause wind loading to be greater in some directions [16]. The effects of wind on a tall structure are divided into static, dynamic, and aerodynamic effects. A static effect is independent of time whilst a dynamic analysis try to capture a change in the system's response during a period of time. The dynamic response of a tall building depends on its structural stiffness, mass, damping, and building form. There are dynamic interaction phenomena caused by wind action such as flutter, galloping, vortex shedding, torsional divergence and gust load [14].

3.1 Wind loads

In this section, the equations for wind actions according to Eurocode 1 [16] are presented.

The average wind velocity, v_m, at height z above ground is decided by

$$v_m(z) = c_r(z) \cdot c_0(z) \cdot v_b \tag{3.1}$$

where v_b is the basic wind velocity, $c_r(z)$ is the roughness factor, $c_o(z)$ is the topography factor and k_r is the terrain factor. These are determined in the following way

$$v_b = v_{b,0} \cdot c_{season} \cdot c_{dir} \tag{3.2}$$

where $v_{b,0}$ is the fundamental value of the basic wind velocity, c_{season} is the seasonal factor and c_{dir} is the directional factor.

$$c_r(z) = k_r \cdot \ln(z/z_0) \quad \text{for } z_{min} \leq z \leq z_{max} \tag{3.3}$$

where z_0 is the roughness length, z_{min} is the shortest height according to table 4.1 in Eurocode [16] and z_{max} is 200 meters.

$$c_r(z) = k_r \cdot \ln(z_{min}/z_0) \quad \text{for } z \leq z_{min} \tag{3.4}$$

$$k_r = 0.19 \cdot (z_0/z_{0,II})^{0.07} \tag{3.5}$$

where $z_{0,II}$ is 0,05 meters for terrain type II.

The standard deviation of the turbulence component of wind velocity, σ_v, can be received according to

$$\sigma_v = k_r \cdot v_b \cdot k_l \tag{3.6}$$

where k_l is a turbulence factor with the recommended value 1.0.

This gives the turbulence intensity, l_v, at height z as

$$l_v(z) = \sigma_v / v_m(z) \tag{3.7}$$

The peak velocity pressure, q_p, at height z is then calculated through

$$q_p(z) = [1 + 7 \cdot l_v(z)] \cdot 1/2 \cdot \rho \cdot v_m(z)^2 = c_e(z) \cdot q_b \tag{3.8}$$

where ρ is the density of air, $c_e(z)$ is the exposure factor and q_b is the basic velocity pressure.

The wind load acting on the building with consideration to its shape becomes

$$w_{tot} = q_p(z) \cdot c_{p,tot} = q_p(z) \cdot (c_{pe,D} - c_{pe,E}) \tag{3.9}$$

where $c_{p,tot}$ is the total pressure coefficient, and $c_{pe,D}$ and $c_{pe,E}$ are the pressure coefficients for the external pressure on the facades perpendicular to the wind action.

3.2 Frequency distribution of wind loads

The knowledge of which frequencies the excitation force includes is crucial when performing dynamic analyses. This means that the frequency distribution of the wind load needs to be defined. The way a structure reacts to a certain excitation load could vary a lot depending of what material it is made of, its form, and point where the load is acting.

The wind load is often acting in the low frequency range between 0.01 and 10 Hz as seen in figure 3.1 [16]. Normally the wind spectrum has its amplitude peaks at frequencies lower than 1 Hz and will therefore be of more importance to higher buildings where the first eigenmodes are excited in that frequency range [17]. Tall buildings generally have lower first eigenmodes, n_1, than lower buildings according to $n_1 = 46/h$, where h is the building height [16]. The global structure is deflecting the most in the first eigenmode and is therefore of great importance when designing

a building. The general wind power spectral density according to Eurocode [16] is shown in figure 3.1.

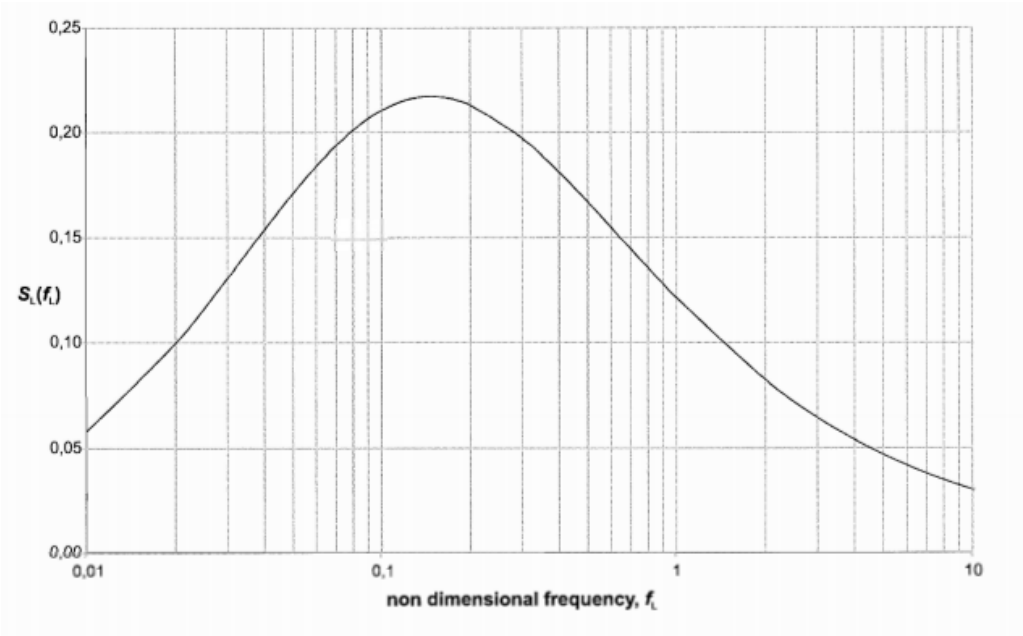

Figure 3.1. The wind power spectral density according to Eurocode [16], where $S_L(f_L)$ is a non dimensional term over the wind density.

Different wind spectra are shown in figure 3.2. The wind spectra are gathered partly from Eurocode [16], and partly from wind turbine tests [18]. The idea here is to obtain both realistic values of the vibrations and sound pressure levels, but also to analyse when an extreme wind spectra could cause sound pressure levels in the auditory threshold.

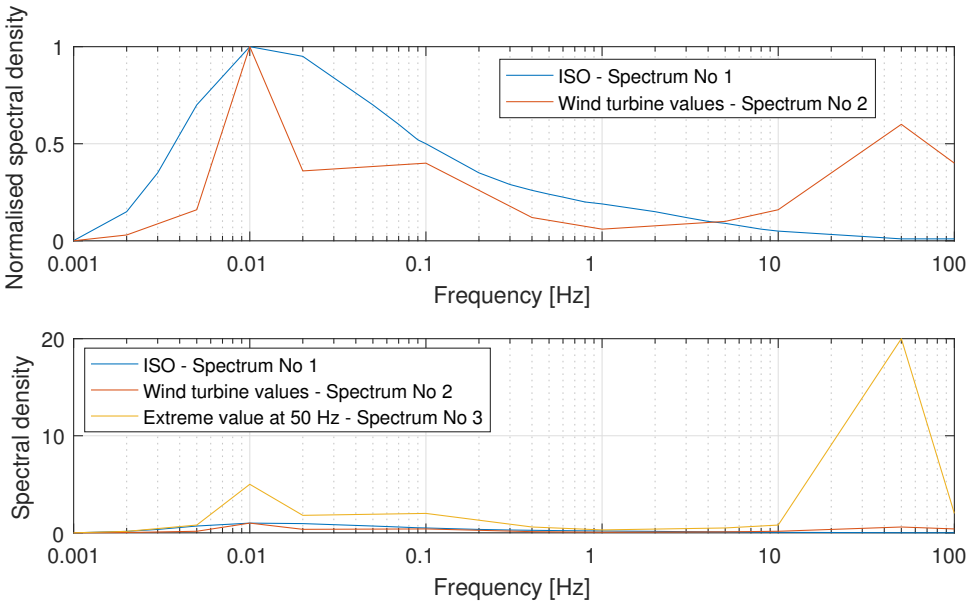

Figure 3.2. Wind spectra with different spectral density. The spectra are varied in the parametric study according to table 6.13.

The blue wind spectrum curve is obtained from [16]. The values in the curve include the frame of the wind spectrum and the frequencies between are interpolated in Abaqus. Data of a measured wind spectrum could give more specific data over every frequencies. The orange and yellow curves show unrealistic wind spectra and are only made to be able to test when the audio threshold will exceed. These curves could simulate effects from turbulence which may include a higher frequency spectra.

A more detailed wind spectrum could be obtained by carrying out measurements. Measurements of the specific wind speed over time are often performed when wind turbines are analysed [17]. Examples of wind turbine measurements can be found in [18]. The wind speed over time could then be transformed to the wind density over specific frequencies by use of Fourier analysis. The wind load could be expressed as a harmonic load with different amplitude in every frequency. The amplitude, A, is therefore frequency-based and could be inserted in the following formula

$$\mathbf{f}(\omega) = A\cos(2\pi f_i t) \tag{3.10}$$

where f_i is the excitation frequency and t is the time.

Wind induced sound is not only radiating from structural vibrations but also from *vortex shedding*, which occurs when wind flow separates by sharp edges. Previous studies show that noise can appear by the friction between elements if a building is set into motion. When measuring facades or other specific construction parts, more complex methods need to be performed. The construction part is then placed in a wind tunnel and is tested to obtain reasonable sound levels. Today there are no good tools to model acoustical phenomena of this kind [19].

4

Governing theory

This chapter summarises important theory applied in this thesis. It includes theory related to sound, vibrations, structural dynamics and finite element theory.

4.1 Acoustics

The term acoustics comprises the science of small pressure waves in air, i.e. sound, and often also structural vibrations. Sound are mechanical vibrations that propagate in an elastic medium. Different medium give different propagation speed, c, which in air and ambient conditions is approximately 340 m/s. c_{air} varies according to

$$c_{air} = 331.4 \left(1 + \frac{T[^{\circ}\mathrm{C}]}{2 \cdot 273}\right) \tag{4.1}$$

The wavelength, λ, depends on the propagation speed and frequency, which in air can be defined as

$$\lambda = \frac{c}{f} \tag{4.2}$$

The frequency, f, is the number of sound wave cycles per second, and its wait is Hertz [Hz].

Two sorts of sound transmission are usually discussed: *structure-borne sound* and *airborne sound*. When measuring the insulation between a construction part, the impact sound insulation or the airborne sound insulation is of interest.

Structure-borne sound describes the vibrations in solid structures, which are induced by direct impact, such as footsteps or machinery, e.g. on the floor, as seen in figure 4.1. The sound that radiates in the material creates vibrations which then get audible if they are in the audible human hearing range. Different types of excitation sources will affect the structure differently depending on which frequencies that the source includes and which impact the source have [11].

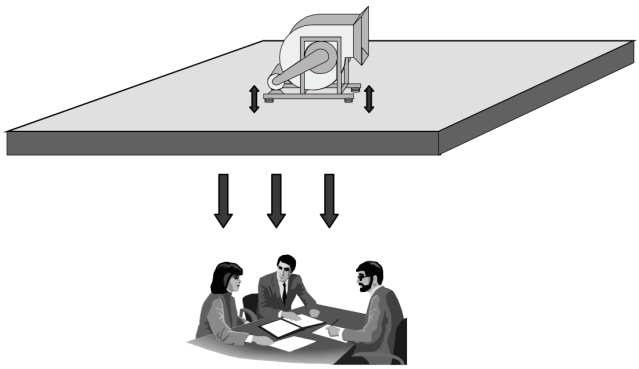

Figure 4.1. Structure-borne sound [1].

Airborne sound describes how sound is propagating in the air. This sound could be induced by a radio, a speech, or other sound travelling by air. The airborne sound could also hit obstacles or elements causing them to vibrate. As an example, the vibrations could transmit through a wall and cause noise on its other side. This should, however, still be distinguished from structure-borne sound, since there is no direct impact between the source and the obstacle, see figure 4.2. In acoustics, a difference is made between airborne and structure-borne sound due to the different behaviour. In contrast to a solid material where many different wave shapes can occur, there is no shear strength in air and therefore only compressional waves can exist [1].

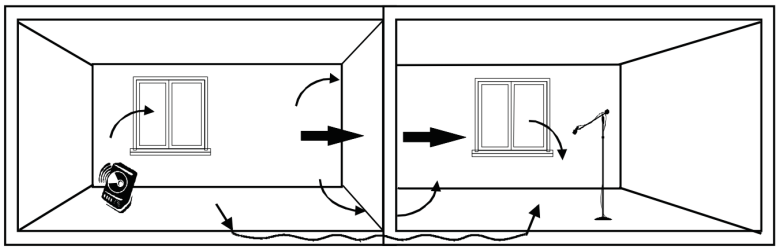

Figure 4.2. Airborne sound [1].

When assessing the transmission or the insulation between two rooms, the transmission coefficient, τ, is used. This factor is describing the energy passing through the material as a ratio between transmitted power, W_t, and incident power, W_i, according to equation 4.3. The transmission coefficient differs for every material and type of surface.

$$\tau = \frac{W_t}{W_i} \tag{4.3}$$

Flanking transmission and direct transmission describe possible paths that the sound could propagate. The sound energy will take the shortest or easiest way when propagating through a partition. This means the energy will go through the weakest

part in the partition. Often these parts are the joints, connections or other uninsulated construction parts. This could be small gaps between the partition, ventilation systems, uninsulated walls, badly connected walls, et cetera [1]. By separating the partition form the surrounding construction the propagation decreases. To obtain good sound reduction, the connection then needs to be well-thought out. Figure 4.6 shows possible transmission paths for both airborne-sound and structure-borne sound. The transmission could also be a combination of both direct and flanking transmission and vise verse.

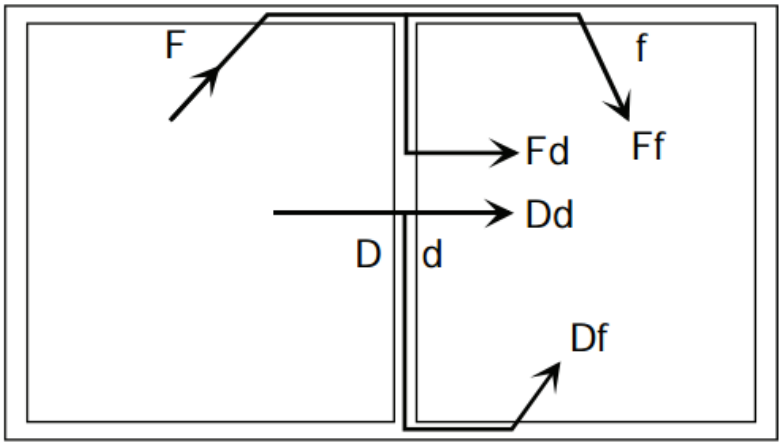

Figure 4.3. Transmission paths [1]. Capital letter indicates the room of the source, and small letters the receiving room. F = Flanking sound, and D = direct sound.

Impedance among many other things is important to get an idea of how much the floor will transmit vibrations and sound. It is described as the relation between the sound pressure, p, and the particle velocity of the sound wave, v, according to [1].

$$Z = \frac{p}{v} = \rho c \tag{4.4}$$

where ρ is the density of the floor and c is the wave propagation speed for the type of wave involved i.e c_L, c_{qL}, c_S, c_B, for longitudinal, quasi-longitudinal, shear, or bending waves respectively, see further about the type of waves in chapter 4.3. The characteristic impedance is $Z_0 = \rho_0 c_0$, where ρ_0 is the density of air and c_0 the speed of sound in air. High impedance can often be found in heavy structures such as concrete slabs and floors. This is therefore a thing to regard in light constructions. One way to increase the impedance for lightweight constructions is to use a shorter span or use elastomers between the storeys [1].

The sound reduction index, R, describes the transmission loss between for example a partition. It is a logarithmic quantity and could be defined as

$$R = 10 \cdot \log \frac{1}{\tau} \tag{4.5}$$

In laboratory measurements it is often presupposed that all the sound energy transmission is going directly through the measured partition, i.e flanking transmission

is well reduced. Due to this, the results are often higher in normally encountered building partitions [1].

The mass law indicates that if the mass or the frequencies are doubled the sound insulation is increased with 6 dB. This means sound isolation easily can be estimated if values are available. Though the mass law only gives an appropriate description in the frequency range lower than the critical frequency [1]. A simple approximation of the mass law could be defined with the transmission loss

$$R_0 = 10 \cdot \log \frac{1}{\tau} \approx 20 \cdot \log \left(\frac{\pi f m}{Z_0} \right) \tag{4.6}$$

Adding the characteristic impedance of air in 20°C, equation 4.6 could be rewritten as

$$R_0 \approx 20 \cdot \log(fm) - 42.5 \quad [dB] \tag{4.7}$$

where f is the frequency and m is the mass.

The transmission loss varies with the frequency. Along the frequency axis, two types of main weaknesses occur: *frequency of first panel resonance* and *coincidence region*. Figure 4.4 shows an overall picture of different phenomena controlling the frequency regions.

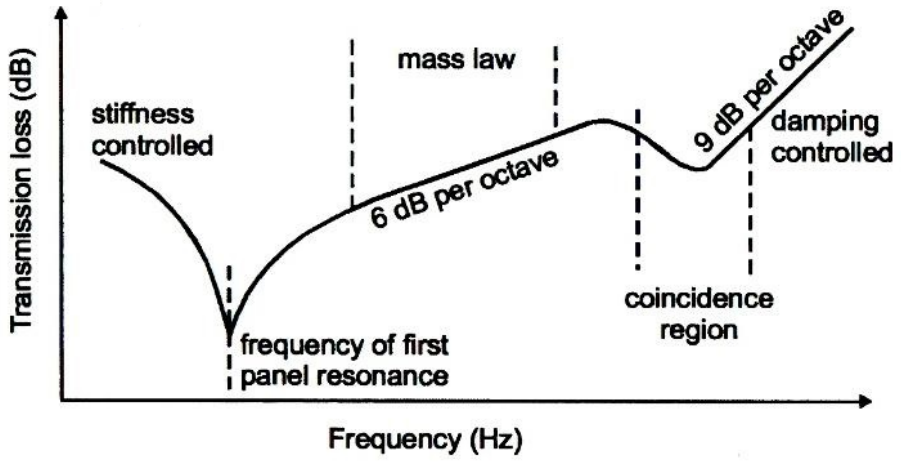

Figure 4.4. Transmission loss depending on frequency region [20].

The first eigenfrequency, or the *frequency of the first panel resonance*, has the largest effect on the transmission loss and is therefore often of interest, including in this master thesis. The first eigenfrequency, f_0, could affect different type constructions, such as leaf walls and double leaf walls which could be determined by

$$f_0 = \frac{1}{2\pi} \sqrt{\frac{s}{m_1} + \frac{s}{m_2}} \tag{4.8}$$

where s is the stiffness per unit area presented in the cavity and m_1 and m_2 are the mass per unit area of the two leaves.

The coincidence effect occurs when the wavelength of the sound in air is the same as for the bending waves in the partition, which depends on the angle of incidence of the waves. The oscillation of the partition will then be amplified and therefore easily transmitted through the partition, almost without attenuation [1]. *The critical frequency*, f_c, is the lowest frequency where coincidence effect occurs and is determined by

$$f_c = \frac{c_0^2}{2\pi}\sqrt{\frac{m''}{B}} \tag{4.9}$$

where m'' is the mass per unit area of the surface and B denotes the bending stiffness [1]. The coincidence effect does, however, mostly affect the higher frequencies and will not affect the results in this master thesis.

4.2 Sound waves in gases and sound pressure level

In inviscid fluids there only exists compressional and longitudinal waves due to no shear motion. When using linear approximations according to [1], the wave equation can be formulated as

$$\frac{\partial^2(r \cdot p)}{\partial r^2} - \frac{1}{c_0^2}\frac{\partial^2(r \cdot p)}{\partial t^2} = 0 \tag{4.10}$$

where r is the distance from the centre of the source to the measured point and t is the time. If analysing one specific frequency the sound pressure in a arbitrary point in the sound field could be obtained with the harmonic solution

$$p(\mathbf{r}, t) = \hat{p} \cdot e^{j(\omega t - \mathbf{k}\cdot\mathbf{r})} \tag{4.11}$$

where $\mathbf{k} = \mathbf{n} \cdot 2\pi/\lambda$ is the *wave number vector* and λ is the *wavelength*.

The pressure could be obtained as a function of time or location at a certain time. Often the oscillatory motion of the sound propagation is of interest. This means that the amplitude of the maximum motions needs to be found. When these values are obtained the root mean square values, RMS could be calculated with

$$\tilde{p}^2 = \frac{1}{T}\int_0^T p^2(x,t)dt \tag{4.12}$$

From equation 4.12 the sound pressure level, SPL, could then be described as

$$L_p = 10 \cdot \log\left(\frac{\tilde{p}^2}{p_0^2}\right) \quad \text{[dB]} \tag{4.13}$$

The reference value, p_0, is equal to $2 \cdot 10^{-5}$ Pa, which is the lowest sound pressure that an average human ear could distinguish.

4.3 Waves in solid media

In difference from fluids, there are several possible types of waves in a solid medium. The different types are quasi-longitudinal wave, shear wave and bending wave. The latter is mostly effecting the sound transmission and will therefor be explained a little more in detail. Figure 4.5 shows the different patterns of the different wave types.

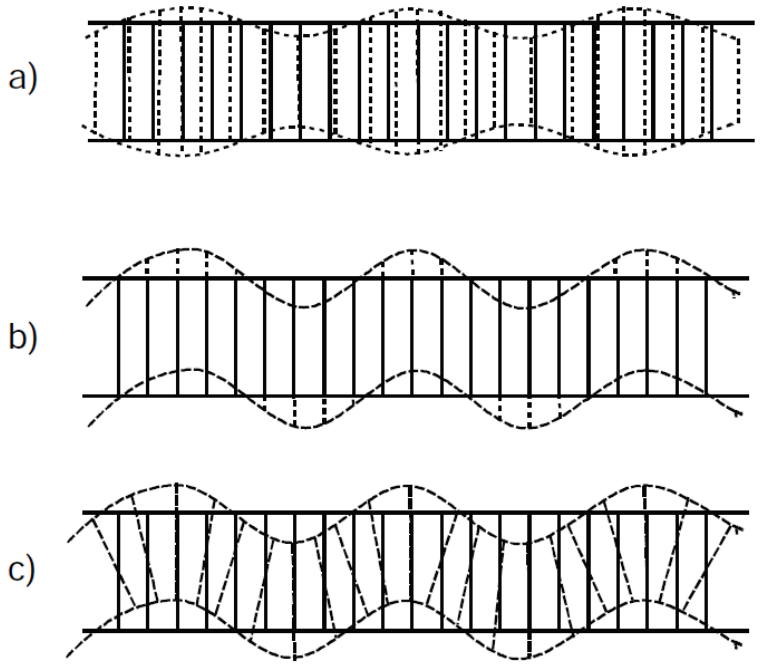

Figure 4.5. Different wave types in solid media. a) shows the quasi-longitudinal wave, b) shear wave, and c) bending wave [1].

Bending waves are of importance when analysing the sound transmission and radiation of buildings. The bending waves dominate in elements like beams and plates, and are easily excited. The particle velocity will propagate in the normal direction of the beams which therefore also leads to a potential sound source which will occur in the normal direction from the beam. Different thickness of the beam will lead to different types of model approaches, thin- or thick plate models. To apply this models in anisotropic materials such as wood, material properties in every fibre direction is needed. If the bending wave length, λ_B, is bigger than six times the thickness of the plate, then the theory of thin plates can be used. The bending wave acts in the dispersive solid medium, which means that the phase speed is frequency dependent. The bending wave length is calculated with equation 4.2 together with the propagation speed, c_B according to

$$c_B = \sqrt{\omega} \cdot \sqrt[4]{\frac{B}{m}} \quad or \quad c_B = \sqrt{hf \frac{2\pi}{\sqrt{12}} c_{qL}} \quad [\mathrm{m/s}] \tag{4.14}$$

where the quasi-longitudinal propagation speed is $c_{qL} = \sqrt{\frac{E}{\rho(1-\nu^2)}}$ and the longi-

tudinal propagation speed is $c_L = \sqrt{\frac{E}{\rho}}$. B denotes the bending stiffness, h is the thickness, ρ is the density and ν denotes the Poisson's ratio [1]. The shear wave propagation speed could be described as $c_S = \sqrt{\frac{G}{\rho}}$ where G is the shear modulus.

4.4 Noise perception

A human hearing is normally said to detect frequencies in the range between 20 and 20 000 Hz [21]. The noise could be divided into physical characteristics and corresponding hearing sensations. The physical characteristics could be defined as sound pressure level, frequency and duration, where the corresponding hearing sensations would be loudness, pitch and subjective duration. Several subjective variables will affect the hearing perception and varies from person to person [22]. According to [23] noise containing tones is more disturbing than noise without tonal components.

For airborne sound and structure borne sound there are regulations according to [24, 3], but they are regulated between a certain frequency range which in some occasions may not be enough. The regulations are set to obtain a healthy sound pressure level and mainly cover frequencies down to 50 Hz, but even though the regulations are fulfilled the noise could still be disturbing.

The human hearing range has different sensitivity in different frequencies. Lower frequencies has less influence than the higher frequencies, see figure 4.6.

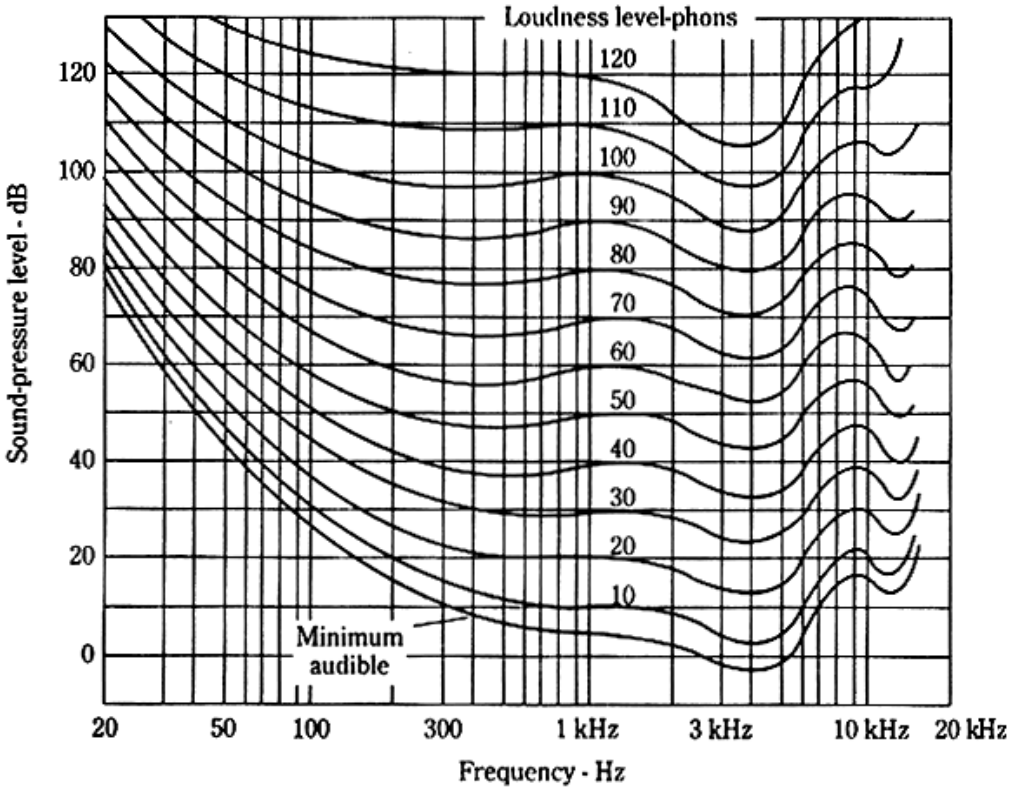

Figure 4.6. Human perception levels of phone curves [21].

4.5 Vibration perception

When a structure is excited it starts to vibrate. Depending on which modes that are exited different structural effects will appear. The vibration amplitude depends on how the structure is excited and how the structure is connected or restricted due to boundary conditions.

According to Juan Negreira [11], the perception is varying a lot depending on age, gender, posture, fitness, type of activity being preformed, attitude and expectations. The perception includes both the physically feeling of vibrations in the ground, and the sound pressure. There are today no regulations for acceptable vibrations, but rather some guidelines [16].

In ISO 10137 [25] perception limits are given in forms of evaluation curves. The figures 4.7a and 4.8 show guidelines of the vibrations for an open-plan office.

Laboratory data from Tamura [26], see figure 4.7b, show the perception threshold at 2% probability.

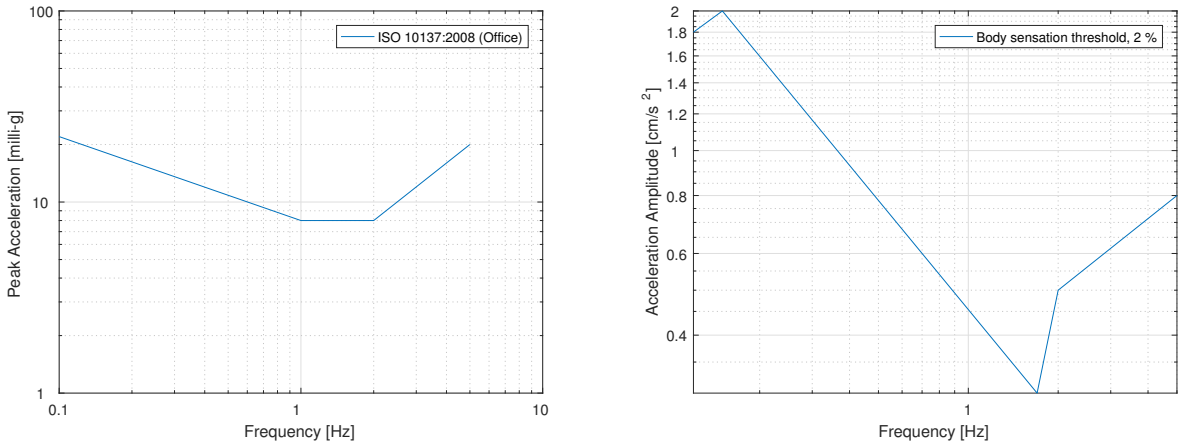

Figure 4.7. (a) Evaluation curve for vibrations in horizontal direction [25]. (b) Body sensation threshold, 2%, for vibrations in horizontal direction [26].

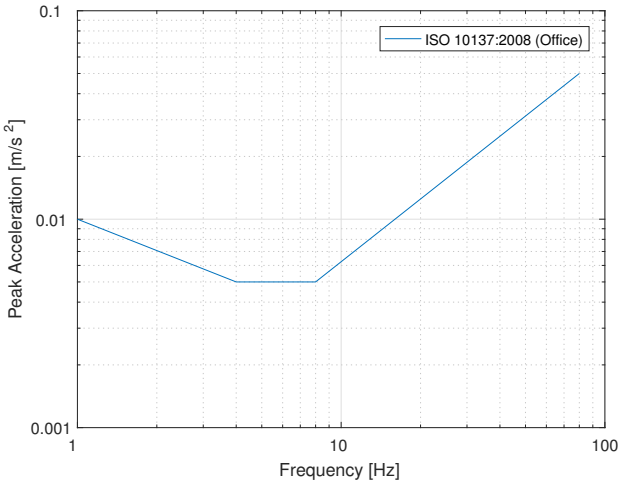

Figure 4.8. Evaluation curve for vibrations in vertical direction [25].

4.6 Single-degree-of-freedom systems

The number of unknown, independent variables in a system to define a problem is called degrees-of-freedom, DOF [27]. The easiest way to describe a dynamic system is by a single-degree-of-freedom, SDOF, system. When analysing a structure with different excitation forces, dynamic solutions often get involved. The excitation affects the structure's modes. Each mode has a natural time period and frequency. The natural time period, T, is the time it takes to complete a periodic motion, which depends on the angular frequency, $\omega = 2\pi/\mathrm{T}$. To get an estimation of the vibration in the model, a numerical approach could be used.

A SDOF system normally includes a mass-spring-damper system, which could represent a floor with an applied dynamic excitation force, see figure 4.9.

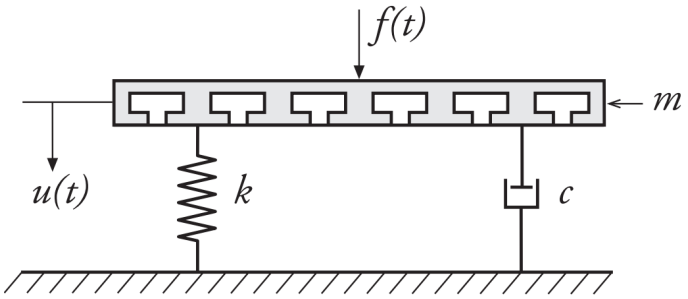

Figure 4.9. A mass-spring-damper SDOF system [11].

The motion of the SDOF system could be described with

$$\mathrm{m\ddot{u}(t) + c\dot{u}(t) + ku(t) = f(t)} \tag{4.15}$$

where m describes the mass, c is the damping and k is the stiffness. u is the displacement, $\dot{u}$ is the velocity and $\ddot{u}$ is the acceleration. f is the vector of the external force acting on the structure. f contains both the boundary vector and the load vector. The displacement in equation 4.15 could be solved by implementing initial conditions [11].

4.7 Multi-degree-of-freedom

Often the system has several degrees of freedom and therefore the multi-degree-of-freedom, MDOF, system is introduced, see figure 4.10.

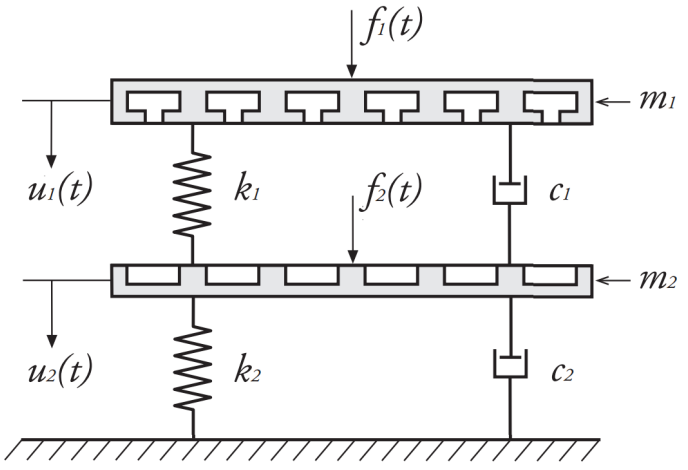

Figure 4.10. A two-DOF system: a mass-spring-damper MDOF system [11].

.

The equation for n-degree-of-freedom is shown below

$$\mathbf{M}\ddot{\mathbf{u}}(t) + \mathbf{C}\dot{\mathbf{u}}(t) + \mathbf{K}\mathbf{u}(t) = \mathbf{f}(t) \tag{4.16}$$

where n is equal to the numbers of degrees of freedom, DOFs. $\mathbf{M}$ describes the mass matrix and $\mathbf{C}$ is the damping matrix. $\mathbf{K}$ is the global stiffness matrix. This depends on the geometry and the material of the total structure. $\mathbf{u}$ is the displacement, $\dot{\mathbf{u}}$ is the velocity and $\ddot{\mathbf{u}}$ is the acceleration. $\mathbf{f}$ is the vector of the external force acting on the structure. $\mathbf{f}$ contains both the boundary vector and the load vector. The equation can be solved with for example the finite element method [11].

The solutions derives from either a particular equation or a homogeneous equation. *The particular solution* could be expressed with harmonic loading, i.e. *steady state*, with which the load and displacement could then be expressed with a complex functions

$$\mathbf{f} = \hat{\mathbf{f}}e^{i\omega t} \quad and \quad \mathbf{u} = \hat{\mathbf{u}}e^{i\omega t} \tag{4.17}$$

Where $\hat{\mathbf{f}}$ denotes the complex load, and $\hat{\mathbf{u}}$ the displacement amplitude. By inserting 4.17 into 4.16 the equation of motion could be expressed within the frequency domain [11].

The homogeneous solution of the undamped and unloaded DOF could be used to express the dynamic characteristics of the system which is further expressed in the next section.

4.7.1 Undamped systems and natural frequencies

It is important to obtain the natural frequencies to get a knowledge of how the structure will react to forces. Modal analysis of linear dynamic systems is a procedure which with the use of the natural frequencies predicts how the structure will move by an induced load in the terms of mode shapes. The first natural angular frequency could be defined with

$$\omega_n = \sqrt{\frac{k}{m}} \tag{4.18}$$

Hence, the mode shapes symbolise the deformation patterns and they depend solely on the mass and the stiffness of the structure. The natural frequency can be explained as the self-wanted frequency in which the structure starts to vibrate in a certain movement. The lowest natural frequency gives the *fundamental mode shape*. If the induced force includes the natural frequencies the structure reach resonance, $\omega = \omega_n$.

To determine several natural frequencies following equations could be performed. The equation 4.16 could be reformulated with no damping and no force as

$$\mathbf{M}\ddot{\mathbf{u}}(t) + \mathbf{K}\mathbf{u}(t) = 0 \tag{4.19}$$

with the solution

$$\begin{aligned} \mathbf{u} &= A \cdot sin(\omega t) \\ \ddot{\mathbf{u}} &= A(-\omega)^2 sin(\omega t) \end{aligned} \tag{4.20}$$

By substituting equation 4.20 into equation 4.19 it gives

$$\mathbf{K\Phi} = \omega^2 \mathbf{M\Phi} \tag{4.21}$$

When introducing the trivial solution meaning there is no motion of the system, equation 4.21 can be written as a homogeneous system

$$(\mathbf{K} - \omega^2 \mathbf{M})\mathbf{\Phi} = 0 \tag{4.22}$$

When constitute an eigenvalue problem the natural angular frequencies could be solved with

$$det(\mathbf{K} - \omega^2 \mathbf{M}) = 0 \Rightarrow \omega_1, \ldots, \omega_n \tag{4.23}$$

The natural angular frequencies can solve the eigenmodes. Further information is found in [11].

4.8 Damping

Damping is a parameter describing how an oscillating system over time is reducing or preventing the oscillation. The oscillation is reduced due to that kinetic energy from the vibrations transforms into heat. Often damping is of great importance for the structure's behaviour. There are many types of existing material damping such as viscous-, structural/hysteretic-, frictional/coulomb-, and Maxwell damping. Often these parameters are very hard to predict or obtain which have led to a more frequent use of just viscous- and structural damping. Some of the damping ratios for different materials are presented in table 4.1 [28].

Table 4.1. Damping ratio's for complete or part of light weight structures [28].

Type of structure	Viscous Damping Ratio, ζ [%]
Continuous Metal Structures	2-4
Metal Strucure with Joints	3-7
CLT Strucuture with elastomers	6
Wood beam	0.35
Wood beam nailed to plywood	0.5 - 2.5
Wood beam nail and glued to plywood	0.75 - 0.9
Wooden walls with gypsumboards	0.26
Wooden floor with plywood	0.12 - 0.19
Wooden ceilings with gypsumboards	0.19 - 0.3

The viscous damping ratio could be defined as

$$\zeta = \frac{c}{2m\omega_n} \tag{4.24}$$

One common used computation method to set-up the damping matrix **C** is the *Rayleigh-method*. It could be used for both transient and steady-state analyses and is described as

$$[\mathbf{C}] = \alpha_0[\mathbf{M}] + \alpha_1[\mathbf{K}] \tag{4.25}$$

M being the mass matrix and **K** is the stiffness matrix. The coefficients are the pre-defined constants of the system. Seen in this formula, α_0 is controlling the mass damping as α_1 controlling the stiffness [11].

When computing large systems with the Rayleigh method, the coefficients are tricky to obtain. To get valid coefficients in all significant modes an iterative method could be used. The damping ratio in every n-th mode could be formulated as

$$\zeta_i = \frac{\alpha_0}{2\omega_i} + \frac{\alpha_1\omega_i}{2} \tag{4.26}$$

If the damping ratio, ζ, is presumed to have the same effect over all modes that contribute to the dynamic behaviour of the structure, the constants α_0 and α_1 could be written as

$$\alpha_0 = \zeta\frac{2\omega_i\omega_j}{\omega_i + \omega_j} \quad \text{and} \quad \alpha_1 = \zeta\frac{2}{\omega_i + \omega_j} \tag{4.27}$$

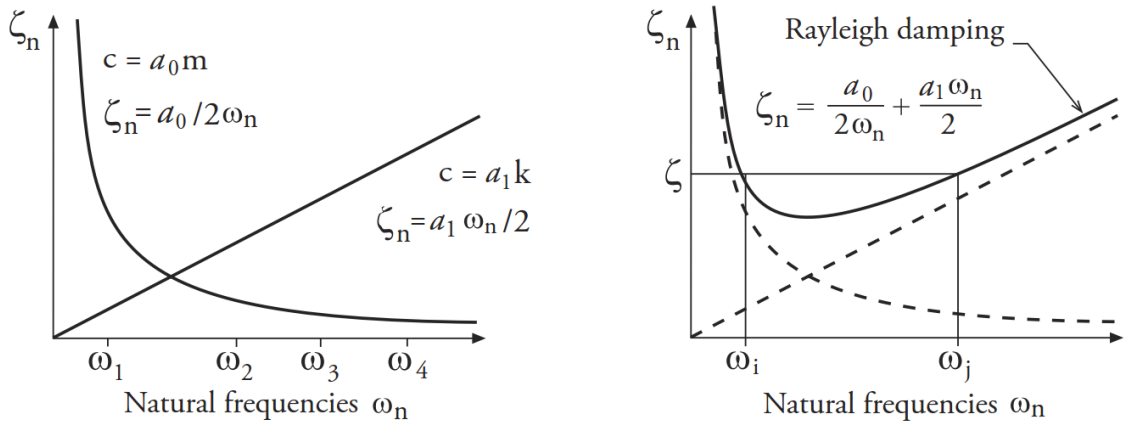

Figure 4.11. Proportional damping due to mass and stiffness, (Left), Rayleigh damping (Right) [11].

Figure 4.11 shows how the adapted damping curve follows both the mass and stiffness damping curve. Although the Rayleigh damping is an approximation of the damping over the mass and stiffness, it has been shown in previous works to be a pretty accurate method [11].

4.9 Finite Element Method (FEM)

4.9.1 Finite element formulation

To describe a problem of linear elasticity a FE formulation with differential equations can be used [11, 27].

The differential equations of motions of a body for three-dimensional problems when assuming small deformations are given by

$$\tilde{\boldsymbol{\nabla}}^{\mathrm{T}}\boldsymbol{\sigma} + \mathbf{b} = \rho\frac{\partial^2 \mathbf{u}}{\partial t^2} \tag{4.28}$$

where $\boldsymbol{\sigma}$ is a vector containing the stresses, $\boldsymbol{b}$ is the body force vector, ρ is the material density, $\boldsymbol{u}$ is the displacement vector, t is the time and $\tilde{\boldsymbol{\nabla}}^{\mathrm{T}}$ is a differential operator matrix [11], given by

$$\tilde{\boldsymbol{\nabla}}^{\mathrm{T}} = \begin{bmatrix} \frac{\partial}{\partial x} & 0 & 0 & \frac{\partial}{\partial y} & \frac{\partial}{\partial z} & 0 \\ 0 & \frac{\partial}{\partial y} & 0 & \frac{\partial}{\partial x} & 0 & \frac{\partial}{\partial z} \\ 0 & 0 & \frac{\partial}{\partial z} & 0 & \frac{\partial}{\partial x} & \frac{\partial}{\partial y} \end{bmatrix};\ \boldsymbol{\sigma} = \begin{bmatrix} \sigma_{xx} \\ \sigma_{yy} \\ \sigma_{zz} \\ \sigma_{xy} \\ \sigma_{xz} \\ \sigma_{yz} \end{bmatrix};\ \mathbf{b} = \begin{bmatrix} x \\ y \\ z \end{bmatrix};\ \mathbf{u} = \begin{bmatrix} u_x \\ u_y \\ u_z \end{bmatrix} \tag{4.29}$$

After carrying out the matrix multiplications of equation 4.28, the weak form is obtained by multiplying with an arbitrary weight function, $\mathbf{v}$, and integrating over the body volume, V. By doing an integration by parts using the Green-Gauss theorem, the weak form is obtained as [11]

$$\int_V \mathbf{v}^T \rho \ddot{\mathbf{u}}\ dV = \int_S \mathbf{v}^T \mathbf{t}\ dS - \int_V (\tilde{\boldsymbol{\nabla}}\mathrm{v})^T \boldsymbol{\sigma}\ dV + \int_V \mathbf{v}^T \mathbf{b}\ dV \tag{4.30}$$

The FE formulation of three-dimensional elasticity is retrieved by dividing the body into finite elements and adding information about the displacements, $\mathbf{u}$, and the arbitrary weight function, $\mathbf{v}$. For the displacement vector, an approximation is made according to

$$\mathbf{u}{=}\mathbf{N}\mathbf{a} \tag{4.31}$$

where $\mathbf{N}$ is a matrix with the global shape functions which vary for each type of element and $\mathbf{a}$ is a vector containing nodal displacements for each element in the body [11, 27].

The arbitrary weight function, $\mathbf{v}$, is approximated with the use of the Galerkin method as

$$\tilde{\boldsymbol{\nabla}}\mathbf{v} = \mathbf{B}^{\mathrm{e}}\mathbf{c}\ ;\ \mathbf{v} = \mathbf{N}^{\mathrm{e}}\mathbf{c}\ ;\ \boldsymbol{\epsilon} = \mathbf{B}^{\mathrm{e}}\mathbf{a}^{\mathrm{e}} \tag{4.32}$$

where $\mathbf{B}^{\mathrm{e}} = \tilde{\boldsymbol{\nabla}}\mathbf{N}^{\mathrm{e}}$, $\mathbf{c}$ is a vector with arbitrary constants, $\mathbf{N}^{\mathrm{e}}$ is the element shape function and $\boldsymbol{\epsilon}$ is a vector with the strains within each element [11].

Applying the approximations from equations 4.31-4.32 into the weak formulation, equation 4.30, yields the following FE equations

$$\int_V \mathbf{v}^{\mathrm{T}} \rho \ddot{\mathbf{u}} \ dV = \mathbf{c}^{\mathrm{T}} \int_V \mathbf{N}^{\mathrm{eT}} \rho \mathbf{N}^{\mathrm{e}} \ dV \ \ddot{\mathbf{a}}^{\mathrm{e}} \tag{4.33}$$

$$\int_V \mathbf{v}^{\mathrm{T}} \mathbf{b} d \ dV = \mathbf{c}^{\mathrm{T}} \int_V \mathbf{N}^{\mathrm{eT}} \mathbf{b} d \ dV \tag{4.34}$$

$$\int_S \mathbf{v}^{\mathrm{T}} \mathbf{t} \ dS = \mathbf{c}^{\mathrm{T}} \int_S \mathbf{N}^{\mathrm{eT}} \mathbf{t} \ dS = \mathbf{c}^{\mathrm{T}} \int_{\Gamma_h} \mathbf{N}^{\mathrm{eT}} \mathbf{h} \ dS + \mathbf{c}^{\mathrm{T}} \int_{\Gamma_g} \mathbf{N}^{\mathrm{eT}} \mathbf{t} \ dS \tag{4.35}$$

$$\int_V (\tilde{\boldsymbol{\nabla}} \mathbf{v})^{\mathrm{T}} \boldsymbol{\sigma} \ dV = \mathbf{c}^{\mathrm{T}} \int_V (\tilde{\boldsymbol{\nabla}} \mathbf{N}^{\mathrm{e}})^{\mathrm{T}} \boldsymbol{\sigma} \ dV = \mathbf{c}^{\mathrm{T}} \int_V \mathbf{B}^{\mathrm{eT}} \boldsymbol{\sigma} \ dV \tag{4.36}$$

When creating a FE model several parameters have to be chosen such as the element type, element size, material parameters, boundary conditions, constraints, loads and type of analysing method [29].

4.9.2 Element types

Abaqus offers a variety of element types that for example can be characterised by the family, the number of nodes or the degrees of freedom. Depending on what elements that are used in a model, the certainty of results and performance of simulations are affected. In this master thesis the upper first two families in figure 4.12, solid elements and shell elements, are handled. The number of nodes depends on the mesh element shape and the geometric order, i.e. whether the interpolation from the nodal displacements is linear or quadratic [29], see figure 4.13.

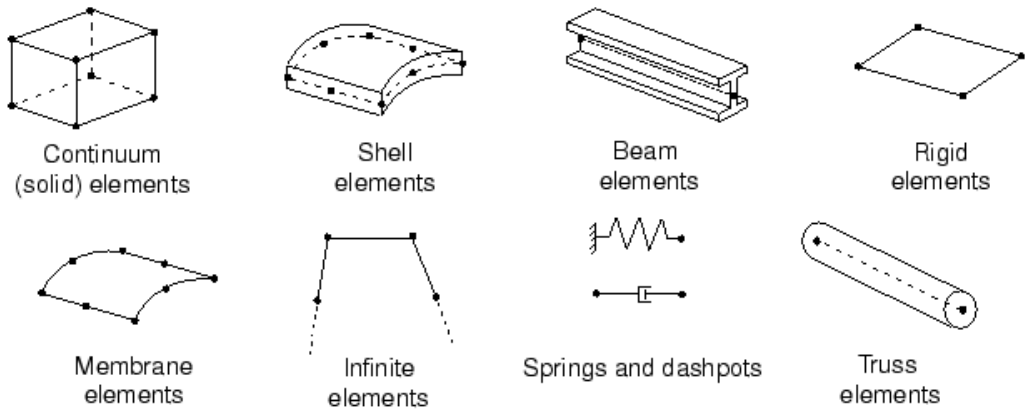

Figure 4.12. Examples of Finite Element Families [29].

(a) Linear element (8-node brick, C3D8)

(b) Quadratic element (20-node brick, C3D20)

Figure 4.13. Elements with different number of nodes and order of interpolation. Here is an example of linear element and quadratic element [29].

More about different sorts of elements can be found in literature [29].

4.9.3 Choice of mesh size

In order to compile a model with a functional mesh size, a rule of thumb is that minimum of six to ten nodes should fit per wavelength, λ. For example, when analysing an element with a frequency interval up to 100 Hz in air, as the case in this master thesis, according to equation 4.2, the wavelength is 3.4 m. If dividing the wavelength by the minimum number of nodes 3.4/6, the maximum mesh size becomes 0.56 m. Hence, with this example, a mesh size below 0.56 m needs to be chosen to estimate an approximately good model.

4.9.4 Correlation and validation

A decision making parameter or parameters must be chosen when comparing various models or when comparing a model with measurements. Those parameters will depend on the application at hand and modalshould be stated along with a tolerance.

A way to compare two models is by looking at their eigenmodes and eigenfrequencies. This can be achieved by looking at two parameters; The Modal Assurance Criterion, MAC and the Normalised Relative Frequency Difference, NFRD.

4.9.4.1 Modal Assurance Criterion (MAC)

The MAC compares two FE-models' eigenmodes and is usually presented in form of a diagram. The diagram shows both models' eigenmodes at the same time and from the plots one can see how well the modes correlate in every different mode. Not just with the correspondent one from the other model but also with every. This is quantified also with a so-called MAC value, which indicate the correlation between two modes. With this method it is easy to find modes that are similar to the ones of the comparing model, which in many cases could be hard to discover, especially in the higher modes.

The eigenmodes denote as Φ_i^a and Φ_i^b and the MAC-value is defined as

$$MAC = \frac{\left|(\Phi_i^a)^T(\Phi_i^b)\right|^2}{\left|(\Phi_i^a)^T(\Phi_i^a)\right|\left|(\Phi_i^b)^T(\Phi_i^b)\right|} \tag{4.37}$$

This is a normalised scalar product of the models' eigenmodes and the values are defined between 0-1. The higher value, the better correlation. A MAC value greater than 90 % is accepted as correlated modes [11, 30]. An example of a MAC diagram is shown in figure 4.14 where the black tiles in the diagonal would present perfect correlation.

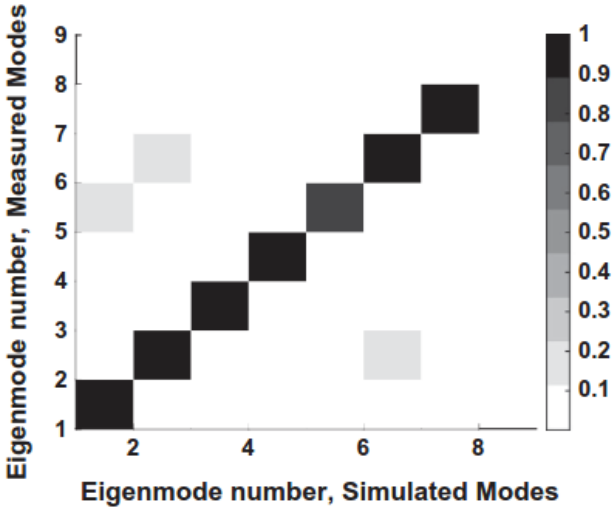

Figure 4.14. MAC-values [**?**]

4.9.4.2 Normalised Relative Frequency Difference (NRFD)

The NRFD complements the MAC-value as a decision making parameter for our FE models. The MAC-values only present the mode shapes and misses therefore the difference in frequencies. Several mode shape could have the same frequencies if different models are made. To assure the frequency difference the NRFD is used. The NRFD gives the eigenfrequency difference in per cent between two models and is defined as

$$NRFD_i[\%] = \frac{\left|f_{ij} - f_{ref_i}\right|}{f_{ref_i}} \cdot 100, \tag{4.38}$$

where the index i denotes the mode number and j denotes the model which is being compared with the considered reference one.

Figure 4.15 shows an example of how the NRFD could look like when several parameters are tested.

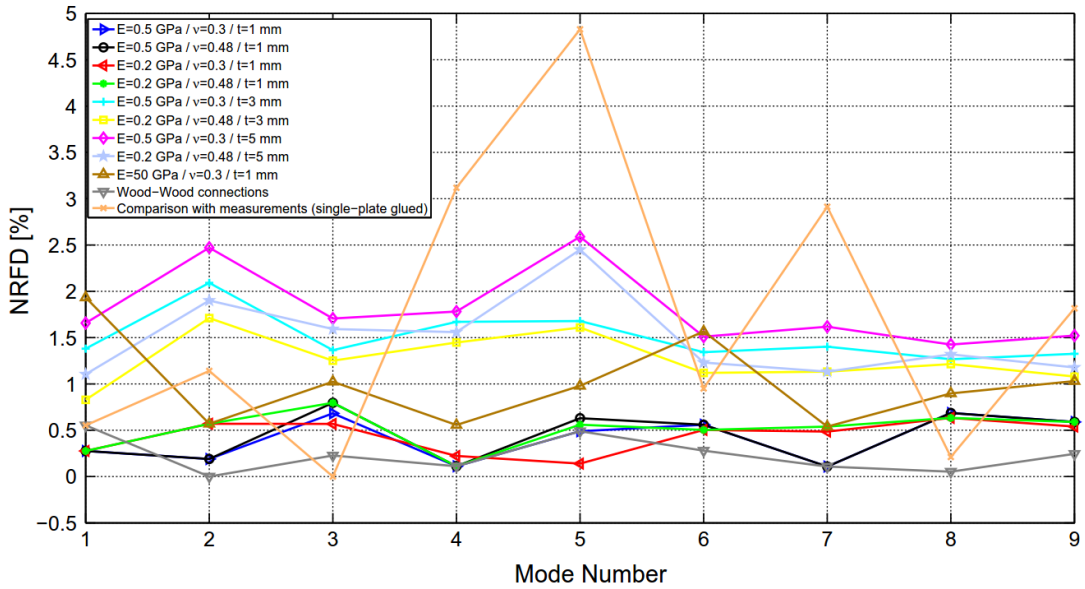

Figure 4.15. NRFD [%] - The curves are compared with the value zero. Several parameters are tested in order to see which model that correlates the most [11].

To justify any accepted difference in eigenfrequency, a comparison to the standard deviation factor of less then 5% is used as a rule of thumb. Therefore an accepted difference in eigenfrequency of 5% is used. Sometimes it is difficult to obtain the limitations and therefore different parameters could be used for various modes.

4.10 Acoustic media

To calculate a model with acoustic media the medium needs to have defined material parameters such as bulk modulus, $K = \rho c^2$, and density, ρ. The part is practically modelled in the same way as any other part. To obtain nodes inside the acoustic media, rather than just on its surfaces, the part needs to be modelled as solid extrude.

The mesh of the acoustic media needs to have the specific acoustic mesh type, whereas the element shape still could be meshed as structured and hex. To calculate the model a steady state method could be performed. If various amplitudes for different frequencies are desired a Abaqus' *steady-state dynamic modal* method could be introduced, which is working for acoustic media.

To be enable values of the acoustic pressure, the acoustic medium needs to have boundaries defined of the surroundings. By default the medium is set as rigid and therefore no boundary conditions need to be specified if the velocities are desired to be zero.

After obtaining the pressure-levels of every node in the medium, an XY-data sheet can be obtained. The values can be extracted into a basic text file which is easy to

use for other post-processing in other programs such as MathWorks MATLAB to obtain other quantities as, e.g. SPL.

5
Example case building

One of the companies that already is producing multi-storey wood buildings is Michael Green Architecture. In this thesis one of their creations called *Wood Innovation and Design Centre*, WIDC, is used as an example case. The building is eight floors with a total height of 29.3 m and has a total floor area of 4 850 m^2 for office and educational use. The structure is designed in a way to make adding floors easy, and the goal is to be able to make a 30-storey wood building based on the same structural principle.

5.1 Design and construction

Using a core as the structural system, or as a part of it together with outriggers, is a widely used way of construction for high-rise buildings, although often with a steel system [31]. The difference between this building in comparison to most other tall buildings is that the framework and structure are completely made of wood. When constructing the building, prefabricated CLT panels and glued laminated timber were used, which in the existing building is seen in the finish at ceilings, floors and façades [2].

Figure 5.1 shows the principle idea of how the framework is set and how extended floors could be added. The core is placed in the middle as a spine to which the main beams are fixed into.

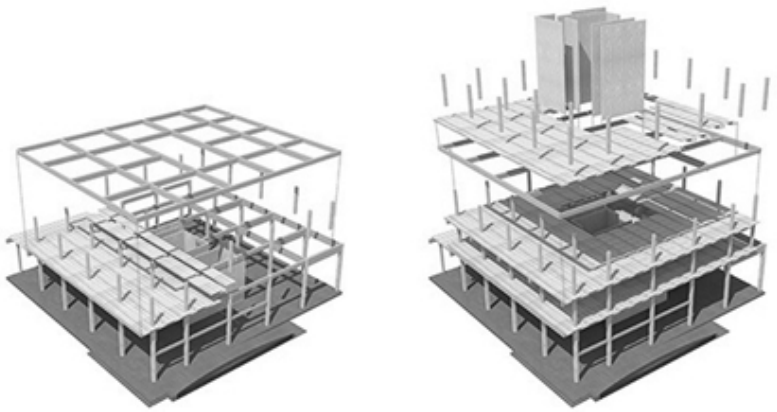

Figure 5.1. Principle idea of the structure [2].

In figure 5.2 the cross section shows the number of layers in the CLT panels and where the cavities for installations are placed. The acoustic insulation and a principle sketch of the regular outer column distributions are seen as well.

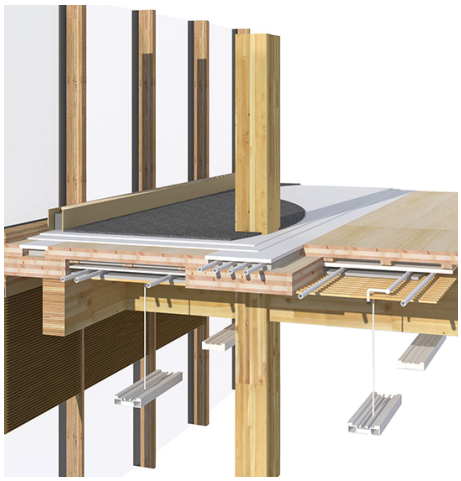

Figure 5.2. Principle of floor structure [2].

The positioning of the lower CLT panels, beams, columns and room volume without walls are shown in figures 5.3a and 5.3b. In figure 5.3a an unsymmetrical distance between the CLT panels is found adjacent to the façade. To obtain any symmetry a shifted break in the middle CLT panel is defined. The approximated symmetry part used in chapter 6 could be found in figure 5.3b.

(a) **(b)**

Figure 5.3. (a) Principle of interior [2]. (b) Symmetry of floor part. Original picture [2]

6

Modelling method - Finding an equivalent shell model

This chapter describes the procedure of the modelling phase. The main idea is to come up with some sort of procedure to help modelling wood multi-storey buildings in an accurate and time efficient way. This is done by thoroughly comparing different modelling techniques and drawing conclusions.

In addition, to estimate the accelerations and sound pressure levels in the construction, a finite element model of the building described in chapter 5 is analysed and recreated. The program Abaqus is used to create the model. Matlab is used as a complementary tool to obtain certain quantities of interest such as SPL. The modelling approach phase is shown step by step in figure 6.1.

Firstly, the building is divided into parts, i.e. walls and floor, modelled and meshed using solid elements. These parts are then used as reference objects, both in terms of mode shapes and frequencies. Subsequently the equivalent model using shell elements is created in order to save computational cost. Then, mesh convergence studies are carried out for both the parts and the global model. The sound pressure level caused by vibrations is finally analysed. The frequency range of interest is below 100 Hertz.

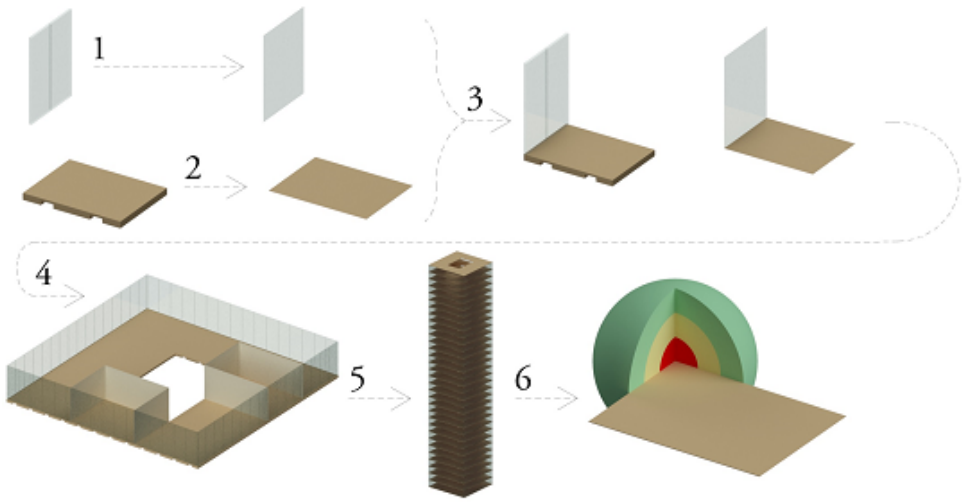

Figure 6.1. The modelling approach step by step.

The steps in figure 6.1 can be explained as:

1. Begin with finding an equivalent shell-based wall model by comparing it with the corresponding solid-meshed, consequently more computationally heavy, one.

2. Continue with comparing solid floor and shell floor parts.

3. Assemble these two parts into a wall-floor part and compare, once again, solid part and shell part.

4. After the wall-floor part is assembled the building model is assembled. Interior walls are added to isolate an acoustic media.

5. An estimation of the rooms where the most severe vibrations would occure is made by carrying out an eigenvalue analysis in the assembled model.

6. Air is included in the worst exposed rooms found in (5). The sound radiation from the walls and floors into the room is calculated to get the average sound pressure level in the rooms.

Note that in the following section a procedure to obtain equivalent shell models to solid models is described. The equivalent junction will eventually be assembled to form the complete building. However in this process, the core of the building has not be taken into account when determine the equivalent shell models. This is why the equivalent thickness and properties of the smeared glass-wood exterior wall may seem a bit unrealistic, as they are considered to be load-bearing. In chapter 7, the core will be added.

6.1 Step 1 - Wall

A large part of the reference building has a glass façade, therefore the exterior wall section is considered as a mixture of glass and wood, a smeard equivalent stiffness being then considered instead. A symmetric part of the wall is chosen to eventually ease the assembling of the more advanced model.

The wall thickness is set to 0.12 m approximated from drawings in figure 5.3a. This value could be smaller and have many different material properties. The width of a single wall element is set to 1.5×3.9 m^2. Four wall elements are combined to make a wall piece with the same width of the floor slab, i.e. W$\times$H = 6×3.9 m^2, seen in figure 6.2.

6.1.1 Wall modelled with solid elements

The solid 6×3.9 m^2 wall part is created with three inner dividing columns which vertically split the wall in four parts, as seen in figure 5.3. The wall is fully tied into

the surrounding beams and columns. The columns and beams are not modelled as fixed boundaries to minimise ties and connections. To get a solution which would theoretically approach the analytical one, i.e. when the element size approaches to zero, the element size is set to 0.07 meters, with quadratic interpolation being used. This will eventually be considered as the reference wall case to which an equivalent shell one will be compared with. In figure 6.2 the wall in solid part is modelled.

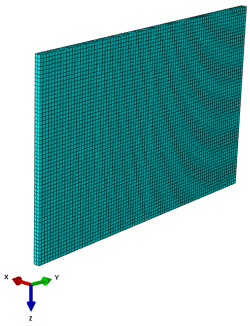

Figure 6.2. A 3D model of the solid wall part. The figure shows an assemble of four wall parts.

The wall is modelled as an isotropic material with material parameters similar to glass as shown in table 6.1.

Table 6.1. Material properties used for a solid wall [32, 33, 34].

ρ	E	ν
[kg/m^3]	[Pa]	[-]
2 500	70E9	0.22

Due to the assumption that beams and columns have fixed boundaries they are not taken into account in the modelling. This solid model is now used as reference when trying to find an equivalent shell structure.

6.1.2 Wall modelled with shell elements

The shell structure model has the same material parameters and dimensions as the solid part.

To be able to work in a more extensive model with shell parts, as the case with the complete building, the interpolation type is set to linear. Different mesh sizes are used to validate the convergence in mesh compared with the solid part. Table 6.2 shows the frequencies in different modes and mesh size. Due to the exterior wall being sectioned into four identical parts with the same boundary conditions, the mode shapes appear the same way in each part of the window and therefore every four mode shape are identical, see figure 6.3, i.e mode 1-4, 5-8, 9-12, and so on. This means the first four modes represent mode 1. In table 6.2 the frequencies of the mode shapes are presented in different mesh sizes.

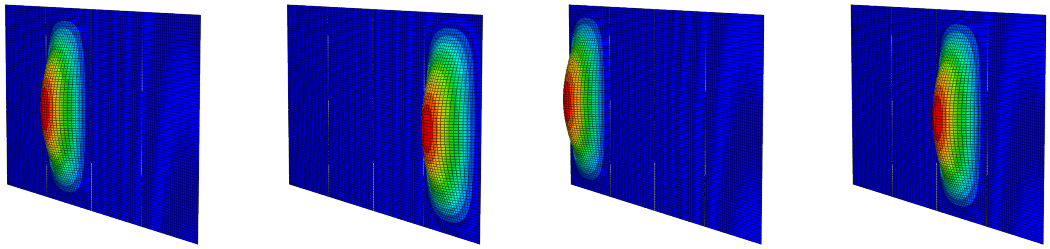

(a) **(b)** **(c)** **(d)**

Figure 6.3. (a)-(d) show the first four mode shapes which are identical for each piece of the wall part and they appear at the frequency 301.05 Hz with a mesh size of 0.07 m. (a)-(d) are therefore representing mode 1.

Table 6.2. Convergence test between shell and solid parts, with the solid part as a reference.

	Frequency [Hz]			
Mesh size [m]:	0.4	0.07	0.05	Ref.
Mode 1-4	356.72	301.05	300.16	300.58
Mode 5-8	394.37	347.18	346.41	347.10
Mode 9-12	481.91	431.89	431.08	431.99
Mode 13-16	649.88	555.88	555.67	556.50

To be able to proceed in the modelling phase, a difference of ±5% in eigenfrequencies between the shell and solid mode shapes is considered acceptable for the NRFD. For the MAC a difference of ±10% is used with the darkest colour representing 98% correspondence, see figure 6.5. In other projects there could be a lower or higher acceptance limit. Further parameters changes can be made in the analysis if some of the eigenfrequencies show a higher difference than the acceptance limit. Another approach to this is to make several models of the same part, each trying to capture acceptable values for different frequency ranges.

When using a NRFD the validation clarifies that the models are correlating. Every mode order from 1 to 16 in figure 6.4 correlates.

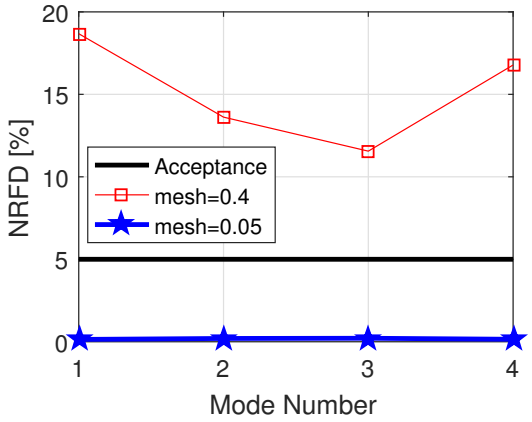

Figure 6.4. NRFD of a shell wall for mode 1 to 16. Due to identical mode shapes, modes 1 to 4 are grouped and referred to as mode 1, modes 5 to 8 as mode 2, etc.

To assure that the mode shapes are correlating, MAC values are retrieved. The pattern between the two models is shown in figure 6.5. The diagonal values are very close to 1, which indicates a good correlation between the two models, but some other modes show similarities to each other. Mode two and three, represented as the four centre pieces, are similar to each other. The last mode has a distinguished value, which could be evaluated more. The fixed boundaries in the solid part complicate the mode shape when trying to translate it into a shell. This leads to different torsional stiffness which makes the mode shapes between shell and solid look different from each other. There is a small difference when comparing the frequencies in NRFD, and the model is therefore accepted.

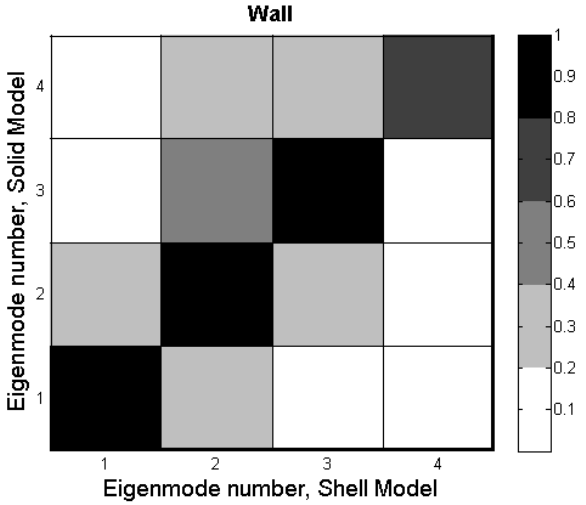

Figure 6.5. MAC values between shell and solid wall. Due to identical mode shapes, modes 1 to 4 are grouped and referred to as mode 1, and modes 5 to 8 as mode 2, etc.

6.2 Step 2 - Floor

Assumptions must be made still keeping in mind to obtain a relatively accurate model. These assumptions are set depending on the project's goals as well as the project's time frame. In this structure there are simplifications regarding the floor.

The floor part is designed in order to save computational time when decreasing the mesh size in the analysis but at the same time keep the floor part in a way so it can be used for symmetry in a storey and therefore not having to use several different floor parts for the model. The symmetric part of the floor is set to 4×3 m^2, where the symmetry is derived from boundary conditions due to stabilising columns and beams according to the reference model. Four of these floor parts together form a slab piece with the area of 8×6 m^2, as seen in figure 5.3b.

6.2.1 Floor modelled with solid elements

To eventually be able to retrieve the SPL existing in a room, the total area of the vibrating parts radiating into the same room is needed, and therefore four of those parts are merged into one part, see figure 6.6.

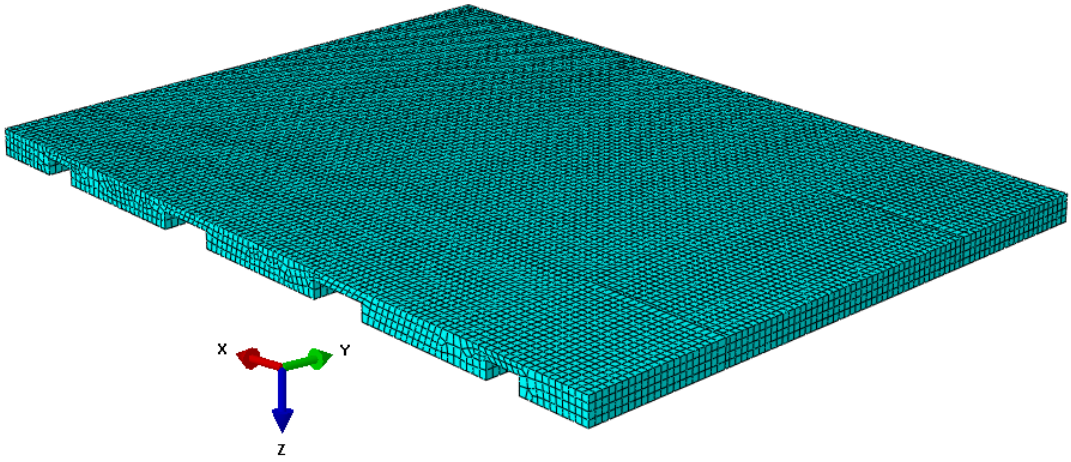

Figure 6.6. Assembled floor of four symmetric parts in the solid model. The part shows one floor slab of the dimensions 6×8 m^2. Global coordinates according to arrows: Red = x-direction; Green = y-direction; Blue = z-direction.

The beams under the CLT panels are modelled as fully fixed connections to the floor slab. Also fixed boundary conditions to the surrounding floor were assumed, which is a simplification that will affect the torsional rigidity and thus the eigenfrequencies and mode shapes. This is done due to see deflection of the floor in an individual symmetric part when analysing the eigenfrequencies and eigenmodes.

The solid floor part is set as a reference floor to which other simplified models, i.e. shell models, will be compared with and has a mesh size set to 0.065 meters. By

using this mesh size and a quadratic geometric order it is believed that this yield a solution close enough to the analytical one. Element shape is set to hex.

The floor is constructed with CLT panels, meaning that the orientation of each layer must be taken into account. The thicker CLT beams is set to have 5 layers plus 3 layers in the thinner CLT part. The thickness of the floor is varying depending on distance to the core. Additional CLT layers are used in every other part and the material properties are put so that the direction with the highest Young's modulus, i.e. E_1, is put parallel to the beams, along the y-axis in the global orientation according to figure 6.6. The thinner, upper layer part is made as one continuous floor.

Tie constraints are used on the surface between the thicker and thinner CLT parts. The thinner part is working as a master surface due to larger area. This means all slave surfaces, i.e. the beam-looking CLT parts seen at the bottom in figure 6.6, will strictly follow the displacement of the master surface.

The reference parts will only be compared in terms of eigenmodes and eigenfrequencies.

The material parameters used in the model are seen in table 6.3.

Table 6.3. Engineering constants, solid [35, 36, 11].

ρ [kg/m^3]	E_1 [Pa]	E_2 [Pa]	E_3 [Pa]	ν_{12} [-]	ν_{13} [-]	ν_{23} [-]	G_{12} [Pa]	G_{13} [Pa]	G_{23} [Pa]
432	8500E6	350E6	350E6	0.2	0.2	0.3	700E6	700E6	50E5

Due to orthotropic parts in different directions the section is set as composite material with specific thickness and stiffness directions, see table 6.4.

Table 6.4. Layer thickness, solid.

Thin CLT	
Layer thickness [m]	Orientation Angle [°]
0.033	0
0.033	90
0.033	0

Thick CLT	
Layer thickness [m]	Orientation Angle [°]
0.034	0
0.034	90
0.033	0
0.034	90
0.034	0

When using non-isotropic parts an orientation compared to the global model is needed for every part.

6.2.2 Floor modelled with shell elements

Variable tests are made by aiming at finding an equivalent single flat shell part to simulate the solid part which is used as a reference model. The reference model is compared in terms of eigenfrequencies and mode shapes. Controlled parameter tests are made when comparing both models. Convergence tests with the NRFD and MAC-values is performed of the different material properties. The results of the material parameters which results in an equivalent shell model to the solid one are shown in table 6.5.

Table 6.5. Engineering constants, shell.

ρ [kg/m^3]	E_1 [Pa]	E_2 [Pa]	E_3 [Pa]	ν_{12} [-]	ν_{13} [-]	ν_{23} [-]	G_{12} [Pa]	G_{13} [Pa]	G_{23} [Pa]
370	8500E6	600E6	350E6	0.2	0.2	0.3	700E6	700E6	50E5

Table 6.6. Layer thickness, shell.

Shell CLT	
Layer thickness [m]	Orientation Angle [°]
0.136	90
0.133	0
0.003	90

After proper materials is obtained a mesh size convergence test is performed. The test results being shown in table 6.8. Different properties are used in order to achieve this result. A trial and error method is performed and finally a good match in most of the modes is reached. To secure the missing convergence and the difference in the frequency range, a secondary shell part could be created to fulfil the limitations, though this is not performed due to time limitations.

Table 6.7. Convergence test with shell and solid as a reference.

	Mesh size [m]				
	0.5	0.07	0.05	0.03	Ref
	Frequency [Hz]				
Mode 1	22.976	22.669	22.666	22.664	21.685
Mode 2	36.957	35.290	35.284	35.280**	31.604
Mode 3	53.793	51.644	51.624	51.610*	51.006
Mode 4	58.830	56.454	56.431	56.417***	58.776
Mode 5	63.157	61.257	61.239	61.227	59.453
Mode 6	81.220	78.621	78.596	78.580	76.433
Mode 7	90.501	84.193	84.135	84.097	80.993
Mode 8	98.125	90.972	90.906	90.862	90.062
Mode 9	105.28	98.908	98.850	98.810*	97.273
Mode 10	108.58	103.14	103.09	103.05	102.63

* Eigenmode with mirrored mode shape compared to the reference model

** Difference is above 5 %

*** Eigenmode is diverging

Figure 6.7 shows how the NRFDs vary for every specific eigenmode. The convergence differ at most in mode 2.

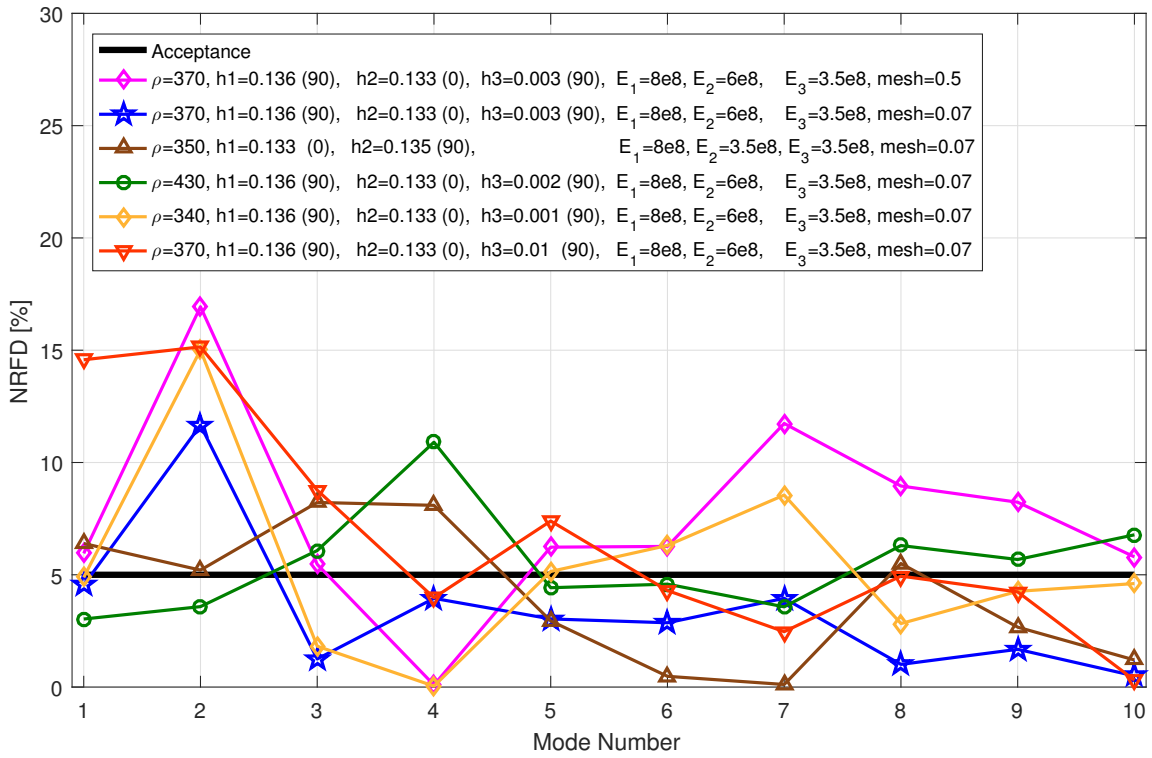

Figure 6.7. NRFD of floor.

The NRFD shows that the parameters according to the blue line has the best correlation with the reference model. Although mode 2 does not fulfil the acceptance criterion of 5%, these parameters are anyway used for the floor due to time issues.

The MAC values in figure 6.8 show good correlations. Some similarities exists between mode 3, 5 and 7, but overall the correlations are good.

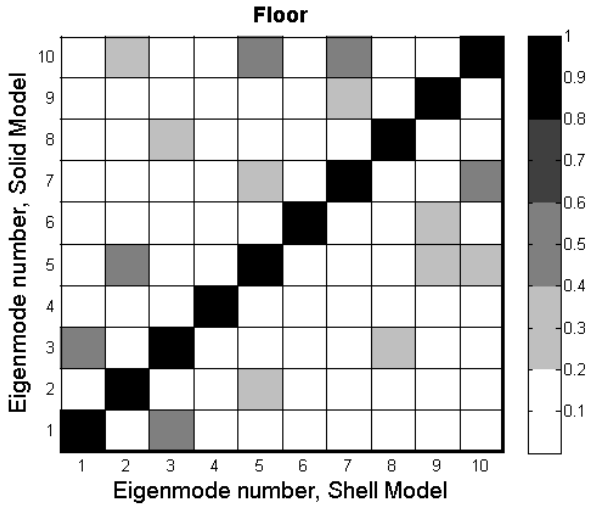

Figure 6.8. MAC values between shell and solid floor.

6.3 Step 3 - Wall and floor connection

When both a shell version of the exterior wall and one of the floor are obtained comparing to their solid equivalents, an analysis with a jointed connection between these parts is done.

The shell model is compared, again, to a solid-mesh model in order to find a shell equivalent.

6.3.1 Wall and floor connection modelled with solid elements

The solid wall of glass established in 6.1.1 and the solid floor according to 6.2.1 are tied together surface to surface at the bottom of the wall width with the floor surface as the master surface and the wall surface as the slave surface. The same boundary conditions as for the single parts are used, i.e. encastred conditions along the three "free" edges on both wall and floor. This may not be a realistic case but the intention here is to show how an equivalent shell would be obtained. Eventually, more realistic BC as well as the core will be considered.

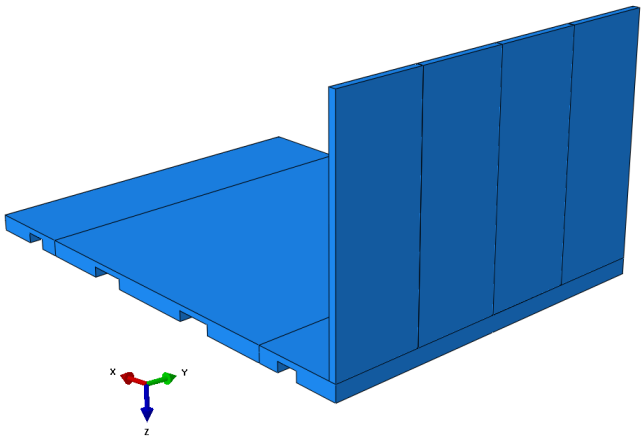

Figure 6.9. Floor of the solid part with jointed connections.

The joint condition between the wall and floor is set to be fixed with same width as the wall part, 0.12 m, along the outer floor edge.

6.3.2 Wall and floor connection modelled with shell elements

In the same way as before, a convergence test is performed to assure the models are correlating. Table 6.8 shows how the eigenfrequencies decrease with a finer mesh size, but with some exceptions. Mode 4 and 10 are diverging according to table 6.8, and mode 2 have a higher frequency difference than the acceptance limit.

Table 6.8. Convergence test with shell and solid as a reference.

	Mesh size [m]			
	0.07	0.05	0.03	Ref
	Frequencies [Hz]			
Mode 1	22.669	22.666	22.664	21.693
Mode 2	35.290	35.284	35.280*/**	31.684
Mode 3	51.646	51.624	51.610	50.997
Mode 4	56.454	56.431	56.417***	59.191
Mode 5	61.258	61.239	61.227	59.512
Mode 6	78.622	78.596	78.580	76.720
Mode 7	84.193	84.135	84.096	81.801
Mode 8	90.978	90.906	90.862	89.951
Mode 9	98.914	98.850	98.810	97.251
Mode 10	103.14	103.09	103.05***	103.22

* Eigenmode with mirrored mode shape compared to the reference model
** Difference is above 5 %
*** Eigenmode is diverging

In the convergence shown in figure 6.10, different mesh sizes are used. The plot gives the indicator that mode 2 is above the criterion. To fulfil convergence in every mode another parallel model could be used with different material parameters. Due to time limits this is not done.

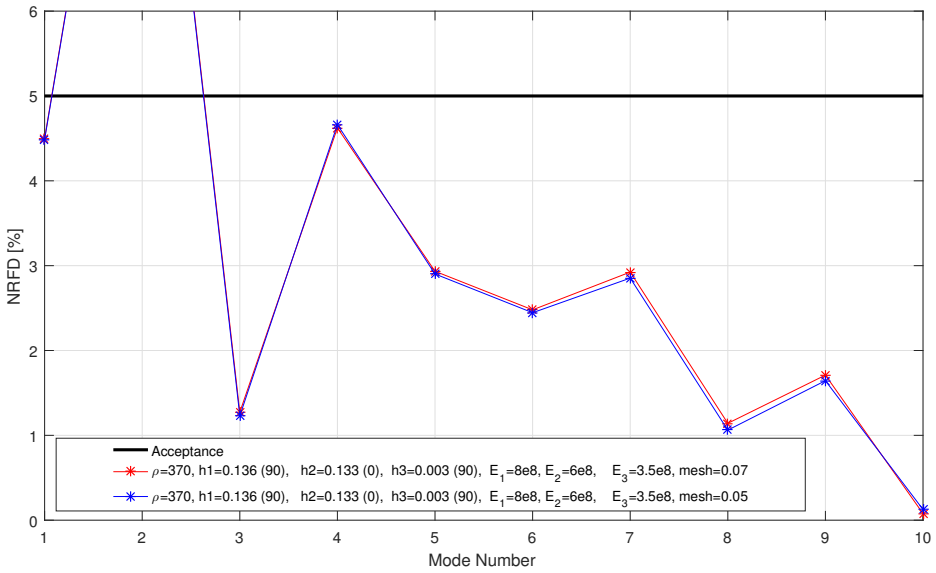

Figure 6.10. NRFD of floor and wall.

MAC values are again controlled to assure the convergence between the mode shapes in the different models. Figure 6.11 shows a good correlation in every mode shape with some minor similarities between other modes. The figure also shows that further parameter tests could be done to obtain even better convergence.

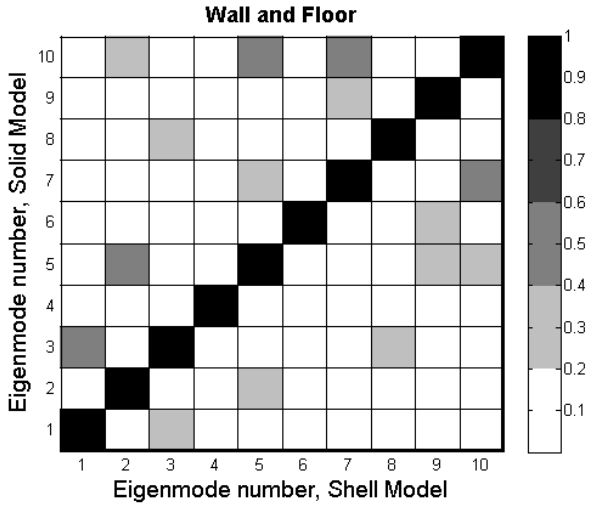

Figure 6.11. MAC values between shell and solid parts of wall and floor connection.

6.4 Step 4 - One storey of the building without core

The previous junction described in section 6.3 is repeated to form a complete floor by tying several of them together. Interior walls are modelled and attached to the surroundings by fixed connections to create several rooms that will contain the acoustic media and thus be able to retrieve SPL created in the room, as described later on in section 6.5. The material of the interior walls is set to be gypsum board with parameters according to table 6.9 and with the thickness of one basic layer of gypsum board, 12.9 mm.

Table 6.9. Material constants for gypsum board [11], used for interior walls.

ρ [kg/m^3]	E [Pa]	ν [-]
848	2250E6	0.3

If an eigenmode analysis is carried out with these properties, the first eigenmodes will affect the interior walls due to their lesser stiffness in comparison to the really stiff exterior wall. A realistic wall does, however, consist of more layers than a gypsum board.

The SPL is not retrieved in all rooms due to time constraints. Just a couple of them were studied, but the procedure that will be shown could be applied to any other room. The chosen rooms were close according to where the highest acceleration values appear on a separate model of 32 floors without rooms. Figure 6.12 shows the design of one floor with two rooms.

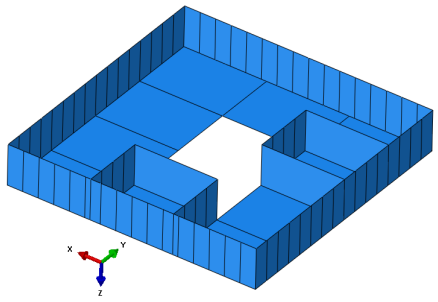

Figure 6.12. Assembled one floor with two rooms without core.

6.5 Step 5 - The building

The desirable building is 32 floors tall, hence 32 storeys are merged together with a top layer of CLT-slab as the roof.

Acoustic medium with the size of one floor slab, i.e. 6×8 m^2, and height 3.9 m is tied together with the surfaces inside of the room. Every floor is modelled with two

rooms as seen in figure 6.12. One room at the time is analysed. The acoustic media have a tie constraint where the media is set to have the master surfaces and the surrounding room surfaces are therefore the slave surfaces. The acoustic media is set to be air and have the same material parameters as air in 20°C, see table 6.10.

Table 6.10. Material constants for air in acoustic media [37, 11].

Density, ρ [kg/m^3]	Bulk modulus, K [Pa]
1.2	138720

The Rayleigh damping method is used for the global model. Depending on the frequency range chosen the damping parameter will be affected a lot. To obtain more accurate damping parameters further parameter tests are made in section 7.1.

6.6 Simplified building without core

To obtain a functional model for the building without a core, tests of varying the boundary conditions are performed. These led to the boundary conditions being set so that the fictive core is fixed in the vertical direction and the bottom slab is encastred. The fictive core boundaries are set in a way to restrict the building from collapsing in the vertical direction because of more realistic movements. If the beams below the floor parts are fixed in the horizontal direction, the global deflection will be zero. The fixed bottom slab is set as restricted in all directions to stabilise the whole building, which is an idealised version of reality. The building is now able to torque and flex in both horizontal directions.

Analyses and a parametric study are performed for this model to obtain indications of the effect for different variable parameters. Note that the latter choice are not realistic given the BC considered assume an infinitely stiff building in the vertical direction of the core, whereas the horizontal stiffness is very weak. That assume that the horizontal stiffness is taken by the exterior wall, its acting as load- bearing. This is why the equivalent exterior wall must be so thick and stiff. In chapter 7 a core is added to obtain more realistic results. However, a parametric study will first be performed on this unrealistic building so as to see parameters that could eventually affect the other model.

6.6.1 Loading case

The applied wind load is varying depending of the height of the building according to wind load shapes in Eurocode [16]. The wind is divided into three pressure loads at different heights and is loaded in the horizontal, positive y-direction. Static wind loading is calculated according to equations 3.1-3.9 for the three different heights.

Since a wind force does not affect all frequencies in the same way, a wind load spectrum is introduced in Abaqus in a tabular manner in the frequency range from 0.001 to 100 Hz. The values for the amplitudes are studied in section 7.1.

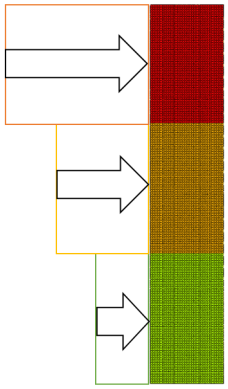

Figure 6.13. A schematic figure over the three pressure loads wind loading is divided into.

The building is to be used as an office space which generates a variable load on each floor. To obtain the total weight of the building, which affects the eigenfrequencies, the variable load is distributed over the floor parts as an added density.

6.6.2 Analyses and obtaining results

By using a modal steady-state dynamics step with a logarithmic scale from the lower frequency 0.1 Hz to the upper frequency 100 Hz, the worst places and floors in the building considering in terms of the accelerations are attained. These places are where analysis with acoustic media is done, for example at the 20th floor as seen in figure 6.14 below. Pressure level values are obtained by firstly taking the average value of all the nodes of the acoustic media and then the absolute of the new obtained value. Acceleration levels are obtained the same way but with using the nodes on the floor surface.

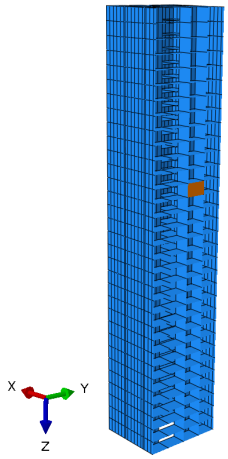

Figure 6.14. Half-section of the building with 32 floors where the highlighted area is the acoustic media in a room on the 20th floor.

First of all, an eigenvalue analysis of two different cases is performed. The results of the eigenfrequencies in a case with normal mass, case 1, are compared with a case with decreased mass, case 4, as shown in table 6.11.

Table 6.11. Eigenfrequencies for case 1 and 4.

Mode	Frequency [Hz] Case 1	Frequency [Hz] Case 4
1	1.0913	1.3011
2	1.0947	1.3046
3	1.6163	1.6164
4	1.6782	1.6783
5	1.7883	1.7883
6	1.7883	1.7883
7	1.7883	1.7883
8	1.7883	1.7884
9	1.7884	1.7884
10	1.7885	1.7885

Due to the absence of a core in this model the eigenfrequencies in case 1 and 4 are not realistic. Later on, a model with a core will be taken into account. Even though the eigenvalues are unrealistic it could be seen that the first eigenfrequency in case 1 is lower than case 4. The weight, stiffness and load distribution will affect the eigenfrequencies as well as the boundary conditions and connections. As the density decreases, such as from case 1 to case 4, the eigenfrequencies increases.

The first two mode shapes are shown in figure 6.15. These modes affect the global structure. Figure 6.16 shows the more complex mode shapes of when local regions are deflecting.

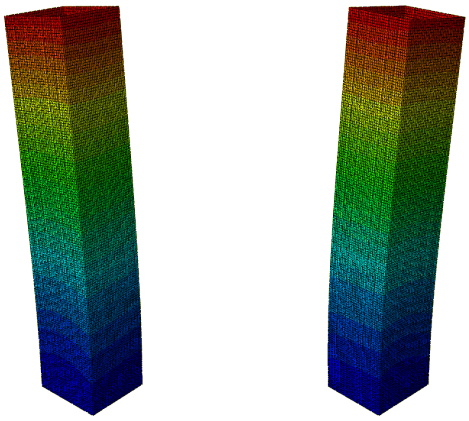

(a) Mode 1 **(b)** Mode 2

Figure 6.15. Mode shapes related to the global structure, i.e. global modes, when an eigenmode analysis is performed.

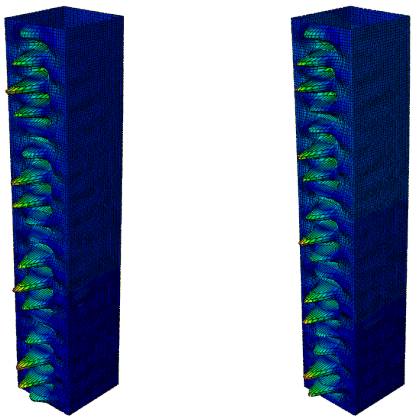

(a) Mode 9 **(b)** Mode 10

Figure 6.16. Local mode shapes affecting several regions at once, making the mode shapes more complex. These shapes are obtained from an eigenmode analysis.

To get an idea of how different parameters influence the results obtained a parametric study is performed. Firstly, an analysis in terms of the predicted normal values of wind load, weight and amplitude is carried out. This will subsequently be referred to as case 1 to which other cases will be compared against. Several different cases are performed and are summarised in table 6.12.

Table 6.12. Description of studied cases.

Case	Description
1	Normal, used as the reference case
2	Changed wind spectrum*
3	Extreme wind amplitude peak at 50 Hz**
4	Lowered mass, i.e. lowered density
5	Lowered damping at higher frequencies
6	Top floor of building in room B
7	Case 6 with changed wind spectrum
8	Case 7 in room A

* An extreme wind amplitude peak over the normal wind spectrum is tested to investigate if the wind could create noise exceeding the audible threshold [21].
** An even higher wind amplitude peak is tested to investigate if the audible threshold will be exceeded.

A more detailed description of every single case with the analysis input parameters is given in table 6.13. A short clarification of the different applied parameters is expressed below.

Figure 6.17 shows the labels of the rooms and the direction of the wind load. The load is applied on one side of the building as seen in figure 6.13, which for the sake of simplicity just shows the principle for one floor.

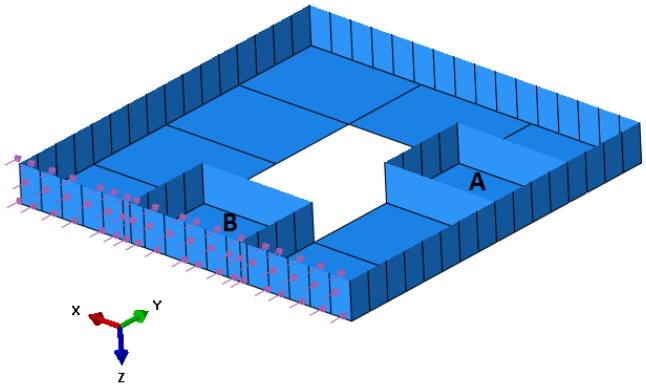

Figure 6.17. The placement of the rooms with their index, A and B, and the direction of the wind load at +Y.

The different parameters that are tested since they could affect the results are density, room placement, type and range of damping, and wind amplitude spectrum. The room placement is varied between two locations at the same floor, A and B, according to figure 6.17, and between floor 20 and 32. As previously mentioned, these room placements were made based on the maximum acceleration levels occurring at the floors when a frequency sweep was performed. The damping is set to Rayleigh damping and varied with different frequency ranges and α_0 and α_1 values, see the

different cases in table 6.13. The wind amplitude is varied by using three different spectra, as presented in figure 3.2. From the parametric study results are given in terms of frequency and pressure level where the bold text symbolises a change from case 1.

Table 6.13. Parameters used for each case where bold text symbolises a change from case 1.

Parameter	Description	Case 1	Case 2	Case 3	Case 4
Density, ρ [kg/m^3]	Wood	1206	1206	1206	**600**
	Exterior wall	2500	2500	2500	2500
	Gypsum	847	847	847	847
	Air	1.2	1.2	1.2	1.2
Room placement	[A/B]	A	A	A	A
	Floor No:	20	20	20	20
Damping	Rayleigh	Rayleigh	Rayleigh	Rayleigh	Rayleigh
	Range [Hz]	0.8-15	0.8-15	0.8-15	0.8-15
	ζ	0.00353	0.00353	0.00353	0.00353
	α_0	0.0337	0.0337	0.0337	0.0337
	α_1	7.1116E-5	7.1116E-5	7.1116E-5	7.1116E-5
Wind amplitude	Spectrum No.	1	**2**	**3**	1
Represented value	Frequency	Yes	-	-	Yes
	Pressure lvl.	Yes	Yes	Yes	Yes

Parameter	Description	Case 5	Case 6	Case 7	Case 8
Density, ρ [kg/m^3]	Wood	1206	1206	1206	1206
	Exterior wall	2500	2500	2500	2500
	Gypsum	847	847	847	847
	Air	1.2	1.2	1.2	1.2
Room placement	[A/B]	A	**B**	**B**	**A**
	Floor No:	20	**32**	**32**	**32**
Damping	Rayleigh	Rayleigh	Rayleigh	Rayleigh	Rayleigh
	Range [Hz]	**0.8-8**	0.8-15	0.8-15	0.8-15
	ζ	**0.05353**	0.00353	0.00353	0.00353
	α_0	**0.4892**	0.0337	0.0337	0.0337
	α_1	**0.0019**	7.1116E-5	7.1116E-5	7.116E-5
Wind amplitude	Spectrum No.	1	1	**2**	**2**
Represented value	Frequency	-	-	-	-
	Pressure lvl.	Yes	Yes	Yes	Yes

6.7 SPL of the model without core

To evaluate the SPL, an extraction of the average absolute values of every nodes in the acoustic media in Abaqus was obtained and post-calculated with Matlab using

the formula according to equation 4.13. The sound curves from the exposed rooms in the model are shown in figure 6.18.

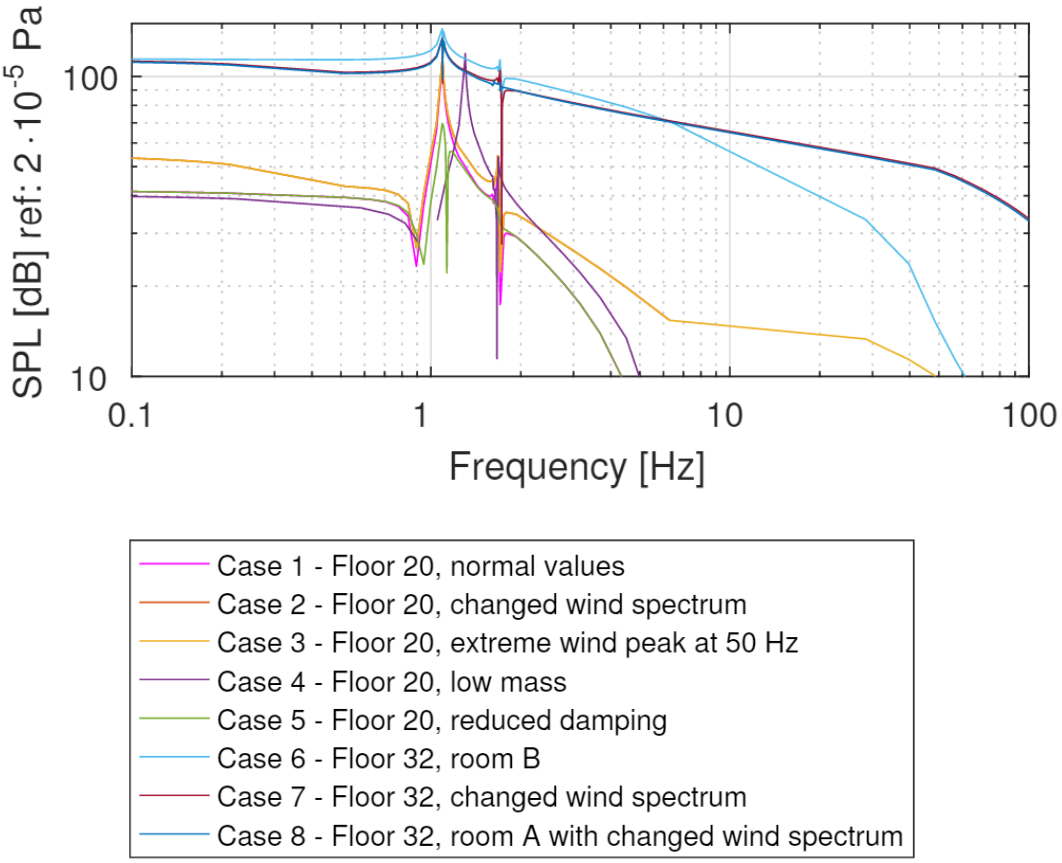

Figure 6.18. Results of the SPL for cases 1-8 compared with the audible threshold [21], seen as the bold, red curve.

Figure 6.18 shows that the audible threshold only is exceeded if an extreme wind spectrum is applied at the worst room placement, see case 7 and 8. Though due to the high stiffness of the model without a core the results from this model should only be taken as an indication of how the parameters relate to each other. Therefor further investigations in the model with a core will be performed with a few of the cases with greatest impact on the SPL.

7

Results and discussion - 32-storey model with core

This chapter covers the results from analyses of the acoustic phenomena and vibrations in the low frequencies induced by wind load in the building model with a core. The intention of the core is to make a more realistic model as the core now beeing the main load-bearing system. Modelled results are compared with regulations. A discussion is held about the model and the results gathered, leading on to a more general discussion for the thesis in section 7.4.

Adding a core to the model and also decreasing the mass and stiffness of the exterior walls enables the core being the main load-bearing system of the building. The core and the changed exterior walls are modelled with the same material parameters, but with different thickness, which implies different total stiffness and mass. The material parameters are set to be isotropic with a stiffness and mass similar to wood. The core and the exterior walls are set to be 0.5 m, respectively 0.02 m thick. The materials are modelled as being isotropic in order to get a stronger stiffness in the core, and as the exterior walls are modelled as an smeared composite material between both wood and glass. The material parameters used for both the core and exterior walls are shown in table 7.1.

Table 7.1. Material properties used for the core and exterior wall [32, 33, 34].

ρ [kg/m^3]	E [Pa]	ν [-]
370	8.5E9	0.22

The floor weight will still be compensated to take the generated variable load, but due to the added core, the floor density is decreased to 900 [kg/m^3].

7.1 Analyses for the building with a core

Based on the results from the analyses described in section 6.6.2, three cases were of more interest to examine the sound pressure level for the model with a core; Cases 3, 6 and 7. As for analysing vibration levels, two more cases were added; Case 9 and case 10. The analysed cases are summarised in table 7.2.

Table 7.2. Description of studied cases for building with a core.

Case	Description
3	Extreme wind amplitude peak at 50 Hz**
6	Top floor of building in room A/B
7	Case 6 with changed wind spectrum*
9	Three floors are analysed with wind spectrum number 2*
10	Three floors are analysed with wind spectrum number 1

* An extreme wind amplitude peak over the normal wind spectrum is tested to investigate if the wind could create noise exceeding the audible threshold [21].
** An even higher wind amplitude peak is tested to investigate if the audible threshold will be exceeded.

Figure 7.1 shows the two room placements and the direction of the wind load for the building with a core. The load is applied on one side of the building, which for the sake of simplicity is shown for one storey according to figure 6.13.

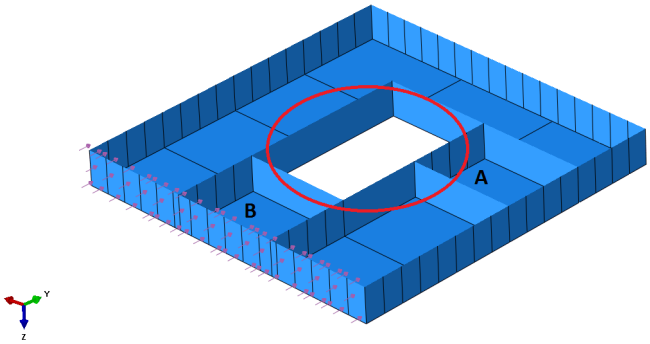

Figure 7.1. The room placements, A and B, and the direction of the wind load at +Y. The red ellipse shows the added core.

First of all, a modal analysis of the building with a core is performed. The results for the eigenfrequencies are shown in table 7.3. The eigenfrequencies are significantly lower compared to the building without a core.

Table 7.3. Eigenfrequencies for modal analysis of the model with a core.

Mode	Frequency [Hz]
1	0.2522
2	0.2945
3	1.0747
4	1.1767
5	1.2778
6	1.7734
7	2.5666
8	2.8154
9	3.0806
10	3.1313

It could be seen that the first eigenfrequency is close to Eurocode's formula when approximating the first eigenfrequency [16]. The frequencies are corresponding to the frequencies in the wind spectra, which probably will affect the vibration level and SPL more than the model without a core. The reduction of stiffness in the exterior walls for the model with a core enable more movements, which affect the eigenfrequencies. The building with a core will also have more weight, which directly affect the eigenfrequencies. Because of the obtained results of the mode shapes and eigenfrequencies, the densities, and thereby masses, of the different materials in the model with a core are kept during all of the tested cases.

The first four mode shapes are shown in figure 7.2. These modes affect the global structure. Figure 7.3 shows the more complex mode shapes where deflections occur in local regions, called local mode shapes.

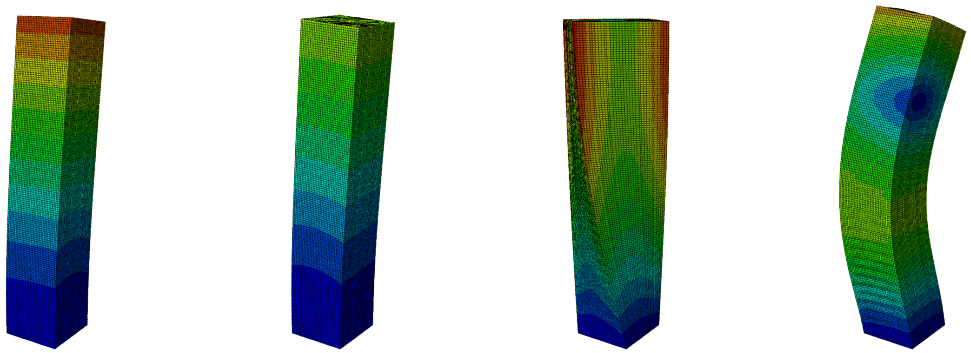

(a) Mode 1 **(b)** Mode 2 **(c)** Mode 3 **(d)** Mode 4

Figure 7.2. Mode shapes related to the global structure when an eigenmode analysis is performed.

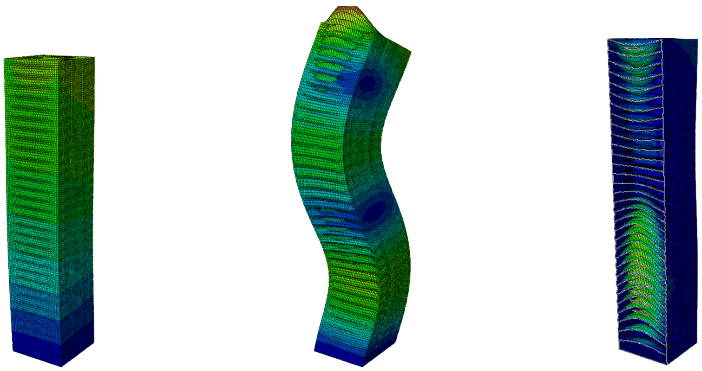

(a) Mode 6 **(b)** Mode 7 **(c)** Mode 9

Figure 7.3. Mode shapes affecting in local regions. A more complex mode shape occur.

Even though no measurements are available to validate the model with a core, these

mode shapes approach the reality much more compared with the model without a core [31, 16].

A more detailed description of all cases with their analysis input parameters is given in table 7.4. A short clarification of the different applied parameters is made in section 6.6.2.

Table 7.4. Parameters used for each case. The represented values differs from case to case from which the results are presented in frequency, pressure levels, and vibration levels in different directions. A/B indicates that both room placements are tested in the case.

Parameter	Description	Case 3	Case 6	Case 7	Case 9
Density, ρ [kg/m^3]	Wood	900	900	900	900
	Exterior wall	370	370	370	370
	Core	370	370	370	370
	Interior wall	847	847	847	847
	Air	1.2	1.2	1.2	1.2
Room placement	[A/B]	A	A/B	A/B	A/B
	Floor No:	20	32	32	2/20/32
Damping	Rayleigh	Rayleigh	Rayleigh	Rayleigh	Rayleigh
	Range [Hz]	0.8-15	0.8-15	0.8-15	0.8-8
	ζ	0.00353	0.00353	0.00353	0.05353
	α_0	0.0337	0.0337	0.0337	0.4892
	α_1	7.1116E-5	7.1116E-5	7.1116E-5	0.0019
Wind amplitude	Spectrum No.	3	1	2	2
Represented value	Frequency	Yes	-	-	-
	Pressure lvl.	Yes	Yes	Yes	-
	Acceleration lvl.	-	Yes	-	Yes
	Acceleration dir.	-	Hor./ver.	-	Hor./vert.

Parameter	Description	Case 10
Density, ρ [kg/m^3]	Wood	900
	Exterior wall	370
	Core	370
	Interior wall	847
	Air	1.2
Room placement	[A/B]	A/B
	Floor No:	20/32
Damping	Rayleigh	Rayleigh
	Range [Hz]	0.8-8
	ζ	0.05353
	α_0	0.4892
	α_1	0.0019
Wind amplitude	Spectrum No.	1
Represented value	Frequency	-
	Pressure lvl.	-
	Acceleration lvl.	Yes
	Acceleration dir.	Hor./vert.

7.2 Sound Pressure Level (SPL)

To evaluate the SPL, the average absolute values of every node in the acoustic media were obtained and post-calculated with Matlab using the formula according to equation 4.13. Curves of the sound pressure levels from the model with a core are shown in figures 7.4 and 7.5.

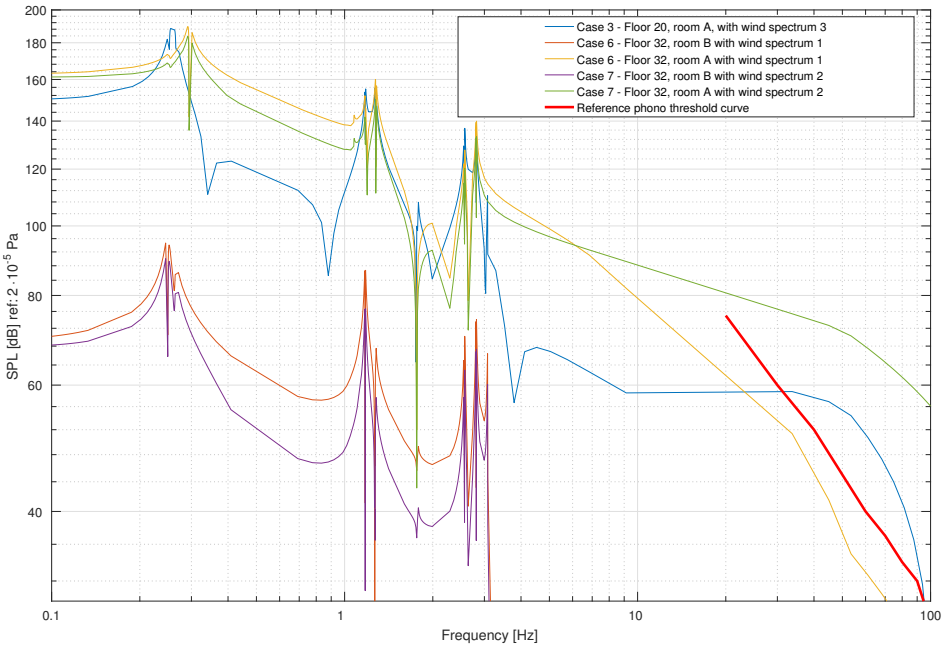

Figure 7.4. Results of the SPL for cases 3, 6 and 7 compared with the audible threshold [21], seen as the bold, red curve.

Figure 7.4 shows the different cases tested for the model with a core. It can be seen that the excitation source mainly affects the structure in the frequency range between 0.1 and 3 Hz. It shows large differences between which room placement that is investigated as seen between case 6, room B, and case 7, room A. The wind spectrum has less effect for this model than showed in the parametric study in the model without a core. When applying wind spectrum number 3, as seen in case 3, the audible threshold is exceeded even if it is investigated at floor 20. Still, if applying wind spectrum number 1 according to Eurocode, it will not exceed the audible threshold at the worst expected room placement, as seen in the yellow curve. The stiffening effect that the core brings into the model enable movements, which affect higher frequencies when the wind load is applied.

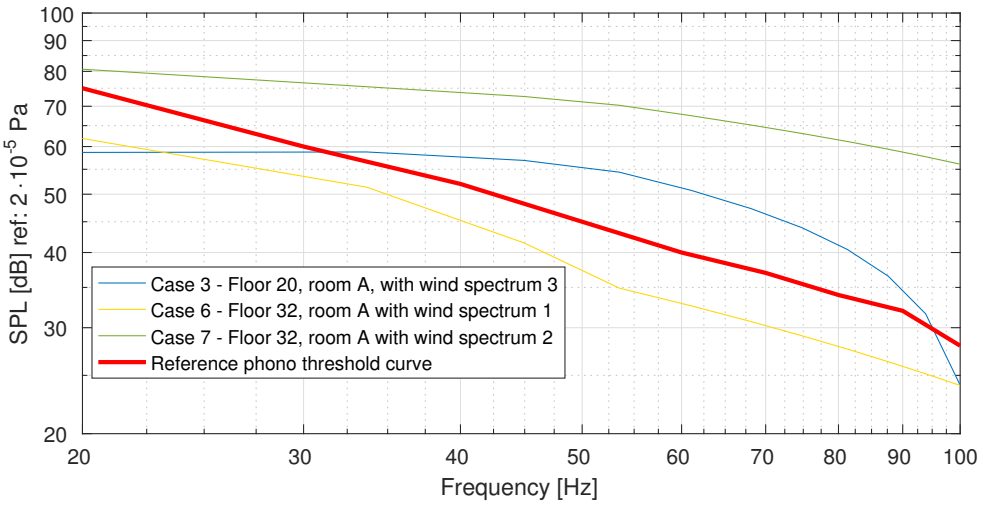

Figure 7.5. Results of the SPL for cases 3, 6 and 7 compared with the audible threshold [21], seen as the bold, red curve.

Figure 7.5 shows more zoomed in results of the effects in the audible threshold of the same cases as 7.4. If very high wind frequency density and low damping parameters is used, i.e α_1-value controlling stiffness is low, the propagated noise does exceed the audible threshold at floor 20 in the worst room placement, seen as the blue curve in case 3.

At floor 32 the sound pressure level may exceed the auditory threshold if the excited wind density is increased at the higher wind spectrum. In the model only fixed connections are modelled, which affect the stiffness of the building and thus to increase the values of the vibrations. Even if the threshold is exceeded in case 3 and 7, see figure 7.5, the model has no interior sound insulation which in a normal construction would reduce the noise considerably. Also, every surface is set to be totally reflective which will also affect the results. Between the range of 30 and 100 Hz it is likely that a normal person would hear the sound from the vibrating surroundings if same conditions as in case 3 and 7 is applied in the worst room placement. At 100 Hz case 7 has a SPL of 56 dB which exceed the audible threshold with 28 dB. The extreme wind spectra 2 and 3 are still fictive values which magnifies the result and therefor the result should be taken as an indication of possible noise.

This points out that, for the model under consideration here, the sound that we hear when the wind is blowing are not likely coming from the wind load itself but rather from rattling of windows, wind hitting the facade or wind turbulence which involving a wind spectrum with higher frequencies like the wind spectra 2 and 3.

7.3 Vibration levels

The following figures show the vibration levels for the three analysed cases; Case 6, 9 and 10.

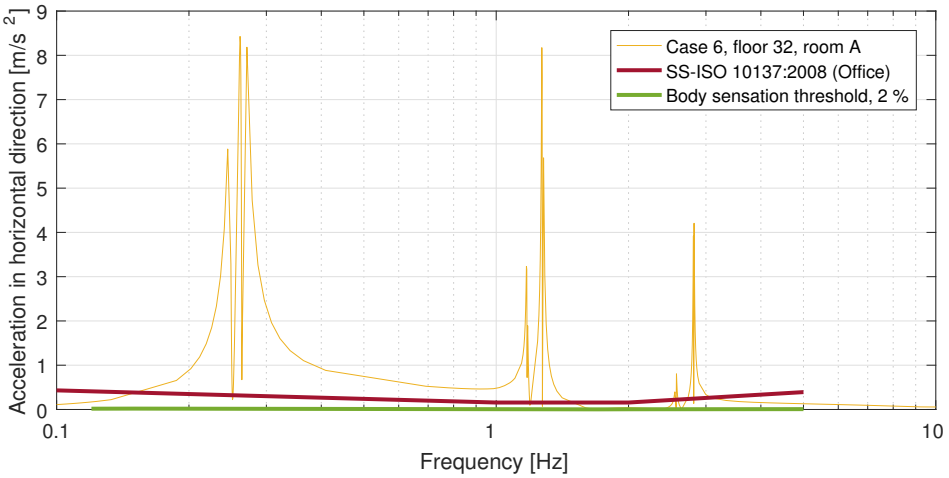

(a) Acceleration for case 6 in horizontal direction.

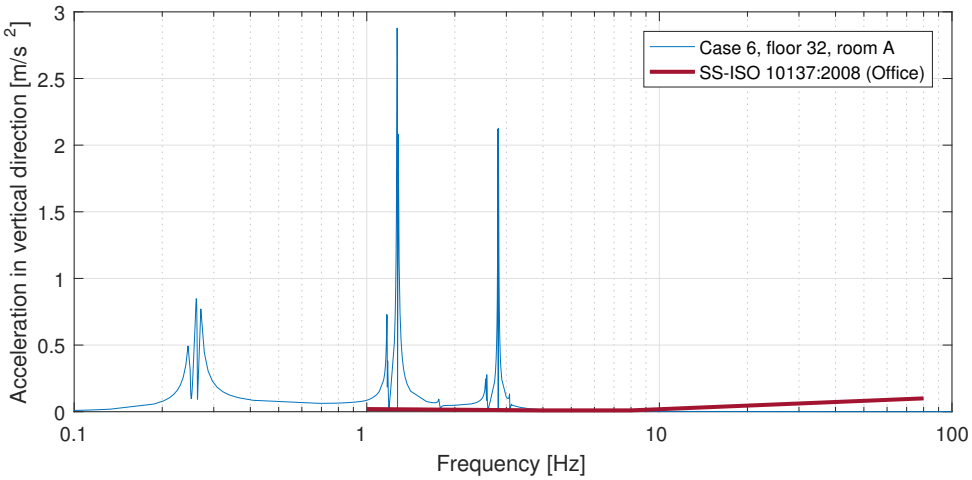

(b) Acceleration for case 6 in vertical direction.

Figure 7.6. Results of the acceleration in vertical direction for case 6 compared with ISO 10137:2008 [25].

Case 6 results in extreme acceleration peaks at the model's eigenfrequencies in both directions, see figure 7.6. This case has a very low damping value, ζ, of 0.353%, which is close to no damping at all. Increasing the damping to approximately 5% for cases 9 and 10 results in accelerations according to figure 7.7 and 7.8.

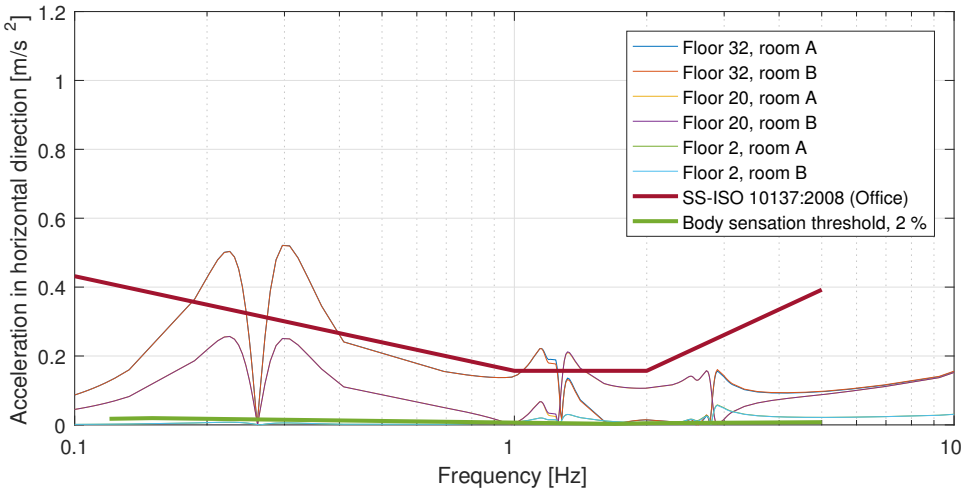

(a) Accelerations for case 9 in horizontal direction.

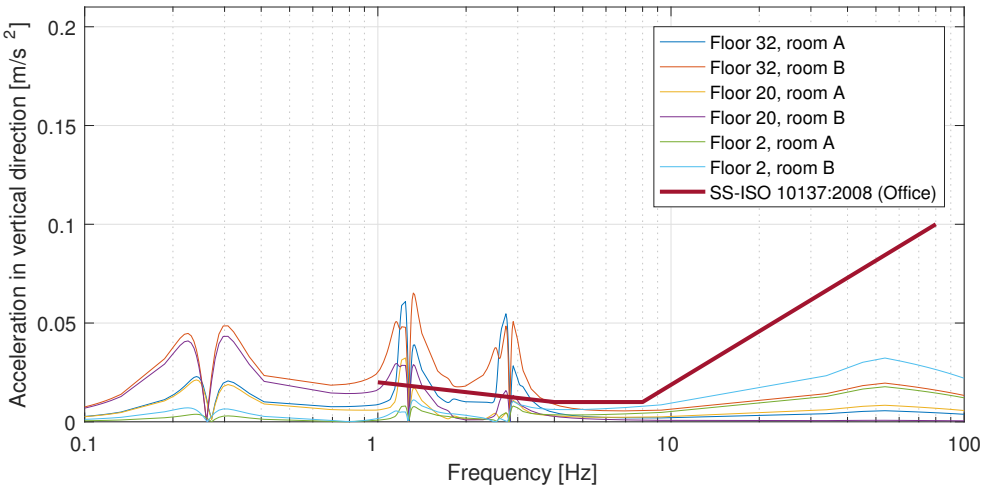

(b) Accelerations for case 9 in vertical direction.

Figure 7.7. Accelerations for case 9 compared with ISO standard [25] and the body sensation threshold, 2% [26], where (a) shows horizontal direction and (b) shows vertical direction. Case 9 has higher damping than case 6 and uses wind spectrum number 2.

The magnitude of horizontal accelerations depends on the floor level, rather than the room placement, according to figure 7.7a. The ISO threshold for office spaces [25] is just being exceeded and only at floor 32.

In the vertical direction shown in figure 7.7b there seems to be a room placement dependency, whereas placement B results in higher acceleration values than placement A. Likewise to the horizontal direction does the vertical direction result in highest acceleration values at the top floor. The ISO threshold is exceeded not only at floor 32, but also at floor 20 for both room placements. The exceeding values are, however, not that far away from the values of the ISO threshold.

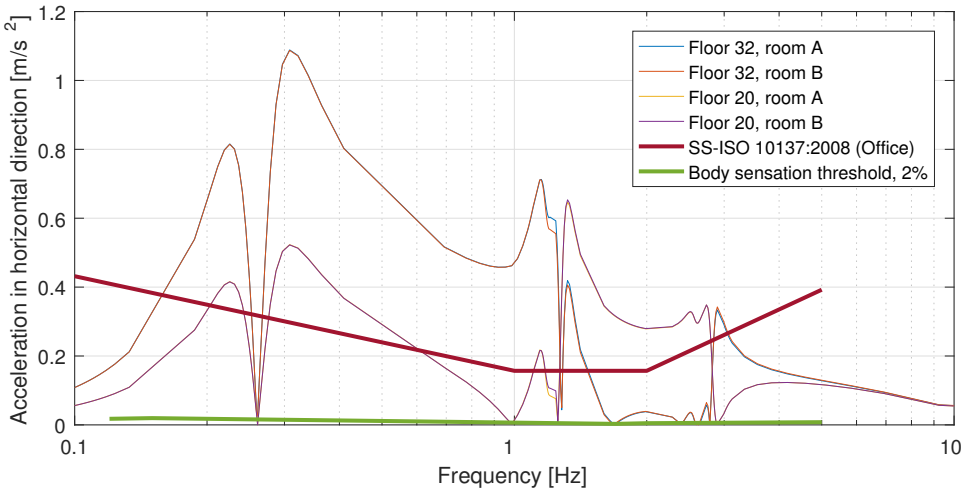

(a) Accelerations for case 10 in horizontal direction.

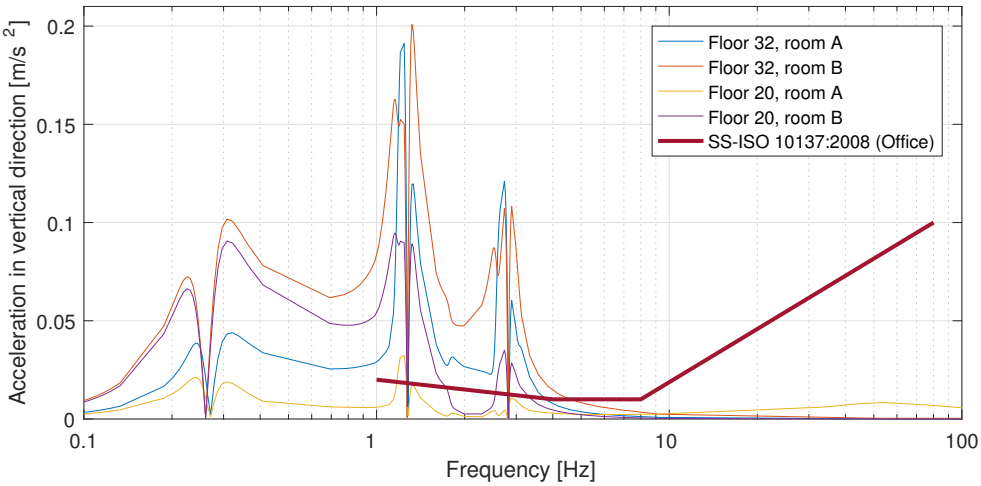

(b) Accelerations for case 10 in vertical direction.

Figure 7.8. Accelerations for case 10 compared with ISO standard [25] and the body sensation threshold, 2% [26], where (a) shows horizontal direction and (b) shows vertical direction. Case 10 has the same damping as case 9, but uses wind spectrum number 1 instead.

Figures 7.8a and 7.8b show higher acceleration values for case 10 than the previous case 9. A change of wind spectrum, as seen between case 9 and case 10, affects the amplitude of the acceleration depending on how well it correlates with the spectrum, but the frequencies at which the acceleration peaks appear remain the same.

In the horizontal direction for all three analysed cases the body sensation threshold 2% is well passed, which indicates that people inside of this building probably will be affected by the vibrations.

7.4 Discussion

In this thesis two 32-storey building FE models are created in order to get sound pressure levels and vibration levels at different locations within the building. The first model was mostly used to perform a parametric study, whereas the second one was to get a bit more credible results. By performing a frequency sweep, the room locations were chosen according to where the highest vibration levels appeared. The results obtained from the core-structured model show that the sound pressure level caused by wind-induced vibrations is not likely to exceed the audible threshold. The vibration levels are, however, exceeding the recommended values and will thereby probably affect the inhabitants. This should be further checked for a model calibrated against measurements in order to generalise this latter statement.

Several assumptions for the modelling, which affect the over-all structure , and thus the results obtained were taken. One of these assumptions is concerning the load-bearing system. The simplified model has a rigid frame structure and boundary conditions set as it was a core-structure. This is an unrealistic structure due to the better boundary conditions, which are set with infinite stiffness in the vertical direction and with too weak stiffness in the horizontal direction. These boundary conditions prevent some of the displacements and movements of the global model. Even though this model is not realistic, analyses are performed just to give indications of the influence of different parameters in the results, in order to gain knowledge about the modelling.

A more realistic model is then created by adding a core to the load-bearing system and decreasing the wall stiffness. However, no comparison with measurements was performed, when setting up the model. The intention of this thesis is partly to investigate possible methods to use when creating a model of reality, not actually creating one. Therefore, the results should be viewed on as indications of an actual case.

Both models were set up using shell elements. A procedure for setting an equivalent shell model from a reference solid one was discussed throughly in chapter 6. This was done to reduce computation times were eventually creating more complicated models. The comparison to validate the shell models was done in terms of NRFD and MAC values when performing modal analyses. When analysing the NRFD and the MAC-values most of the modes fulfils the preset acceptance limit. Even though the majority of the modes between the shell and the solid parts correlate, more material parameters could be tested. An other approach is to combine two or more models of the same part which each fulfil the acceptance limit for different modes. On the downside, using this approach of combined parts will, to a great extent, increase the processing time.

The SPL induced in the selected rooms by the wind load is analysed with a very low damping effect and with no sound insulation added. This affects the SPL significantly and should thereby be taken into account when studying the SPL results.

When analysing the vibration levels in a more realistic case, the damping effect is set to be approximately 5%. This could differ a lot depending on the structure's material and types of joints [28]. The core-structured model is also modelled with fixed connections.

The investigation of room placement could be further developed because of the large impact this has on the results. The SPL is varying a lot depending on which room that is examined. As for the vibration levels, there seem to be a room placement dependency only in the vertical direction. Therefore it would have been good to check possible rooms all over the floor area for each floor. Both the vibration levels and the SPL are most apparent on the top floor.

More wind spectrum tests could have been performed, such as with values from a measured wind load. The effect could influence the vibration peaks depending on if the the wind density correlates with the structure's eigenfrequencies or not.

Moreover, there are plenty of probable sources of noise such as when the wind hits the façade, noise which occur from the wood when it is under compression, small cavities driving air into the building, leakage and rattlings from windows, and so on. These problems could all occur when the wind hits the building, but are very complex and there is no certain way of modelling them. Instead wind tunnel tests could be performed with different parts of the model to get measured sound radiation values [19].

8

Conclusions

The main conclusion that can be drawn from this master thesis for the core model is that it is very unlikely that the sound pressure level will be audible from wind-induced vibrations. Only when using a wind spectra with frequencies up to 100 Hz and with test values obtained from the worst exposed room placement, i.e. where the highest SPL occur, together with very low damping and no extra sound insulation does the sound pressure level exceed the audible threshold in our model. However, this does not imply that wind load can not create noise being audible from other types of interactions such as rattle sound, windows, turbulence due to the building shape, and so on.

The highest sound pressure level is obtained at the top floor of the building in the room furthest away from the applied wind load. The wind amplitude and wind spectrum are of great importance to how the excitation will affect the building. If the wind spectrum does not include frequencies over 20 Hz, no sound pressure level in the audible threshold is obtained in the core-structured model used in this thesis.

Building vibrations could affect humans and might cause different types of negative effects. The results in this thesis show that the vibration levels exceed the guidelines given in [16] in both the vertical and the horizontal directions, which indicates that people inside of this building probably will be affected by the vibrations. Similar to the SPL does the highest acceleration values appear at the top floor, but with room placement closest to where wind load is hitting as the most exposed room for vertical vibrations. No difference in room placement is observed for horizontal vibrations.

The method of creating an equivalent shell model from a solid one proved to be useful in terms of reducing the calculation time. After the comparison with different NRFD and MAC-values the difference is below 5% in most of the modes which shows the equivalence in dynamic behaviour of both models.

To sum it up, a method to set up an equivalent shell model of a 32-storey building from a solid reference model was developed. For the model with the core, both SPL and vibration levels induced by wind load were investigated, which showed that it is unlikely to reach a SPL inside rooms which could be heard by people. However, the vibrations produced could cause displeasure to the inhabitants, since the current guidance values are exceeded by the acceleration levels.

8.1 Further work

In this master thesis several assumptions, as stated in chapter 1.3, were made. To simulate accurate acoustic phenomena is very tricky and depends on nature laws and dynamic problems such as acoustic effects of turbulence in rattles. The combined complexity makes it hard to model in Abaqus. To obtain realistic values of the sound pressure level in a building caused by wind load it could be good to divide the problem into different investigations. As a good start, different measurements of the wind spectra would lead to more accurate amplitudes and realistic excitation frequencies.

If there is an already complete model of a structure, a sub model could be created to analyse the acoustic phenomena and vibration effects more efficiently. The structural behaviour is then already decided and could be inserted to the more detailed model of the acoustic medium.

The joints in this thesis are modelled as fixed connections, which affects both the vibrations and sound pressure level in an excessive way, i.e. creates more vibrations and more noise than it probably would. It could therefore be interesting to add different connections and investigate how they affect the results.

Due to the wind spectra it is likely that the sound pressure level will occur in other ways than vibrations in the structure. A different type of approach would therefore be to model noise caused by compression or leakage through the wall construction. Different shapes of the façade and different stiffness in wood could probably affect the sound pressure level considerably.

During this analysis no measurements were performed. It would be of interest to compare measurements in the existing building with the model parts to ensure the relative error. Calibrating the model with a building in terms of the natural frequency to get more realistic results applying the techniques described in the thesis is advised.

Bibliography

[1] Vigran, T. E. (2008). *Building Acoustics*. Taylor & Francis Group, Abingdon, Oxfordshire, UK, 1st ed. ISBN 978-0-415-42853-8.

[2] Michael Green Architecture. *Wood Innovation and Design Centre*. Available online: `http://mg-architecture.ca/work/wood-innovation-design-center/`. (last access: 2016-09-07).

[3] SIS. (2015). *SS 25267: Acoustics – Sound classification of spaces in buildings – Dwellings (in Swedish)*. Swedish Standards Institute, Stockholm, Sweden.

[4] Svenskt Trä. *Trä som material - Från timmer till planka*. Available online: `http://www.svenskttra.se/om-tra/att-valja-tra/fran-timmer-till-planka/`. (last access: 2016-08-31).

[5] Burström, P. G. (2007). *Byggnadsmaterial: uppbyggnad, tillverkning och egenskaper*, volume 2. Lund: Studentlitteratur. ISBN 978-91-44-02738-8.

[6] Fink, G. (2014). *Influence of varying material properties on the load-bearing capacity of glued laminated timber*. PhD thesis, Graz University of Technology, Zürich: Institut für Baustatik und Konstruktion der ETH Zürich.

[7] Stora Enso. (2013). *CLT - Massive Wood System*. Available online: `http://www.clt.info/en/product/clt-massive-wood-system/`. (last access: 2016-09-01).

[8] Stora Enso. (2016). *Wood: the world's oldest and yet most modern building material*. Building Solutions, Division Wood Products. Stora Enso Wood Products GmbH.

[9] Green Gold Industrial Co., Ltd. *About Wood, Science of Wood*. Available online: `http://www.ggi-myanmar.com/wood/`. (last access: 2016-08-31).

[10] Stora Enso. (2013). *Fördelar med CLT*. Available online: `http://www.clt.info/se/produkter/clt-massivtrasystemet/fordelar/`. (last access: 2016-09-01).

[11] Negreira, J. (2016). *Vibroacoustic performance of wooden buildings: Prediction and Perception*. PhD thesis, 1st ed. Lund: Engineering Acoustics, LTH, Lund

University.

[12] Woodproducts.fi. *Acoustic properties of wood*. Available online: `http://www.woodproducts.fi/content/acoustic-properties-wood`. (last access: 2017-03-05).

[13] Mayo, J. (2015). *Solid Wood: Case Studies in Mass Timber Architecture, Technology and Design*. Fakenham Prepress Solution. ISBN 987-0-415-72529-3.

[14] Mendis, P., Ngo, T., Haritos, N., Hira, A., Samali, B., Cheung, J. (2007). *Wind loading on Tall Buildings. EJSE Special Issue: Loading on Structures*, pages 41–54.

[15] Illustrerad Vetenskap. (2007). *Hur mycket kan höghus svaja? Illustrerad Vetenskap*, (2). Bonnier Publications International.

[16] SIS. (2008). *SS-EN 1991-1-4:2005 Eurocode 1: Actions on structures - Part 1-4: General actions - Wind actions*. Swedish Standards Institute, Stockholm, Sweden.

[17] Jónsson, Ö. (2014). *The dynamic behaviour of multi-story reinforced concrete building in a seismic and windy environment*. Master's thesis, School of Science and Engineering at Reykjavík University.

[18] Van der Hoven, I. (1956). *Power Spectrum of Horizontal Wind Speed Spectrum in the Frequency Range from 0.0007 to 900 Cycles per Hour. Journal of Meteorology*, 14:160–164.

[19] Ploemen, J. C. F., Nijs, L., Pleysier, J. A. and Schipper, H.R. (2011). *Wind-induced sound on buildings and structures*. In *Proceedings of the 13th International Conference on Wind Engineering*, page 8. Multi-Science Publishing, Amsterdam, the Netherlands.

[20] Bies, D., Hansen, C. (2003). *Engineering noise controle, Theory and Practice*. Spon Press 11 New Fetter Lane, London EC4P 4EE. ISBN 0-203-11665-8.

[21] Gatland II, S. D. (2008). *Understanding Acoustics and Sound Control*. Available online: `http://www.aia.org/practicing/awards/AIAB025071`. (last access: 2016-09-08).

[22] Ellermeier, W., Zeitler, A., Fastl, H. (2004). *Predicting annoyance judgements from psychoacoustic metrics: Identifiable versus neutralized sounds, Inter Noise 2004*. `http://mediatum.ub.tum.de/doc/1138382/879380.pdf`.

[23] Vormann, M., Verhey, J.-L., Mellert, V., Schick, A. (2012). *Subjective Rating of Tonal Components in Noise with an Adaptive Procedure*. Available online: `http://www.physik.uni-oldenburg.de/docs/aku/literatur/Vormann/vormann-etal_00a.pdf`.

[24] SIS. (2007). *SS 25268 Acoustics - Sound classification of spaces in buildings - Institutional premises, rooms for education, preschools and leisure-time centres, rooms for office work and hotels (in Swedish).* Swedish Standards Institute, Stockholm, Sweden.

[25] SIS. (2008). *SS-ISO 10137:2007 Bases for design of structures – Serviceability of buildings and walkways against vibration.* Swedish Standards Institute, Stockholm, Sweden.

[26] Tamura, Y. (2009). *Wind and tall buildings.* Wind Engineering Research Center, Tokyo Polytechnic University.

[27] Ottosen, N., Petersson, H. (1992). *Introduction to the finite element method.* Prentice Hall, London, UK. ISBN 978-0-13-473877-2.

[28] Bolmsvik, Å. (2013). *Structural-Acoustic Vibrations in Wooden Assemblies.* PhD thesis, Linnaeus University, Växjö, Sweden.

[29] Dassault Systèmes. (2014). *Abaqus 6.14 Online Documentation - Getting Started with Abaqus: Interactive Edition.* Available online: `http://bobcat.nus.edu.sg:2080/v6.14/books/gsa/default.htm`. (last access: 2016-10-26).

[30] SimuTech Group, Inc. *Modal Testing.* Available online: `http://www.simutechgroup.com/Testing-Services/modal-testing-mac.html`. (last access: 2016-10-26).

[31] Ali, M. M., Moon, K. S. (2007). *Structural Developments in Tall Buildings: Current Trends and Future Prospects. Architectural Science Review*, 50(3):205–223.

[32] Engineering toolbox. *Densities of Solids.* Available online: `http://www.engineeringtoolbox.com/density-solids-d_1265.html`. (last access: 2016-06-20).

[33] Engineering toolbox. *Modulus of Elasticity.* Available online: `http://www.engineeringtoolbox.com/young-modulus-d_417.html`. (last access: 2016-06-20).

[34] Engineering toolbox. *Poisson's ratio.* Available online: `http://www.engineeringtoolbox.com/poissons-ratio-d_1224.html`. (last access: 2016-06-20).

[35] Isaksson, T, Mårtensson, A. (2008). *Byggkonstruktion, Regel- och formelsamling.* Studentlitteratur AB. ISBN 9789144070322.

[36] Serrano, E., Enquist, B. (2010). *Compression strength perpendicular to grain in Cross-Laminated Timber, (CLT).* In *World conference on timber engineering.* WCTE.

[37] Engineering toolbox. *Air Properties*. Available online: `http://www.engineeringtoolbox.com/air-properties-d_156.html`. (last access: 2016-09-22).